Metabolic characteristics of primary muscle cells

of diet sensitive and diet resistant obese patients

Rui Zhang

Thesis submitted to the

Faculty of Graduate and Postdoctoral Studies

In partial fulfillment of the requirements

For the Masters degree in Biochemistry

Department of Biochemistry, Microbiology, and Immunology

Faculty of Medicine

University of Ottawa

ABSTRACT

In the Ottawa Hospital Weight Management Clinic, we have previously identified subpopulations of patients in the upper and lower quintiles for rate of weight loss, and characterized them as 'obese diet sensitive' (ODS) and 'obese diet resistant' (ODR) patient groups, respectively. Skeletal muscle is a major contributor to basal metabolic rate and mitochondrial proton leak in skeletal muscle can account for up to 50 % of resting oxygen consumption. The overall aim of this research is to explore differences in mitochondrial function in human primary myotubes from ODS and ODR subjects.

Subsets of ODS and ODR subjects (n = 9/group) who followed a hypocaloric clinical weight loss program at the Ottawa Weight Management Clinic consented to a muscle (*vastus lateralis*) biopsy. Human primary myoblasts obtained from biopsies were immunopurified and differentiated into myotubes. Mitochondrial function and distribution were compared in intact myotubes from ODS and ODR subjects.

Mitochondrial proton leak was significantly lower ($p < 0.05$) in ODR myotubes compared to ODS myotubes, independent of whether cells were differentiated in low or high glucose medium. In addition, in low glucose medium, ODR myotubes had higher MnSOD protein levels compared to ODS myotubes ($p < 0.05$). However, there were no significant differences in mitochondrial content, mitochondrial membrane potential, cellular ROS levels or ATP content between ODS and ODR myotubes. Overall, our *in vitro* mitochondrial proton leak results are consistent with our previous *ex vivo* results. Future research should examine the possibility that differences in proton leak between ODS and ODR groups may be related to mechanisms of cellular ROS regulation.

Key words: mitochondria, proton leak, uncoupling protein, oxidative stress, obesity

ACKNOWLEDGEMENTS

I would like to thank my supervisor, Dr. Mary-Ellen Harper, for her fundamental support and guidance throughout my M.Sc. studies at the University of Ottawa. She has offered me great research opportunities that allow me to have a better understanding of how the research process works. I would also like to thank Dr. Erin Seifert and Dr. Céline Aguer for their tremendous help with my project as well as for their excellent mentorship and guidance throughout my graduate studies. Finally, I would like to thank everyone in the Mitochondrial Bioenergetics Laboratory for their support.

MITOCHONDRIAL BIOENERGETICS LABORATORY

SUPERVISOR

Dr. Mary-Ellen Harper

CURRENT LABORATORY MEMBERS

Cyril Adjeitey
Dr. Céline Aguer
Ghadi Antoun
Brittany Beauchamp
Linda Jui
Dr. Ryan Mailloux
Melissa Pasqua
Aline Pfefferle
Mahmoud Salkhordeh
Dr. Brianne Thrush
Jian Xuan

PREVIOUS LABORATORY MEMBERS

Amanda Daniels
Adrian Ebsary
Carmen Estey
Cynthia Moffat
Marisa Rossi
Dr. Erin Seifert
Naveen Venayak
Shelinna Xu

I would also like to thank all of our collaborators at the University of Ottawa Heart Institute, the Ottawa Hospital Weight Management Clinic, and the Ottawa Hospital Bariatric Program. Without all of the time and effort individuals from these institutions contributed, these studies would not have been possible.

University of Ottawa Heart Institute

Dr. Ruth McPherson
Heather Doelle

Ottawa Hospital Weight Management Clinic

Dr. Robert Dent
Angelique Blackmore

Thesis Advisory Committee Member

Dr. Ruth McPherson
Dr. Jean-Marc Renaud

TABLE OF CONTENTS

LIST OF ABBREVIATIONS

4-HNE - 4-hydroxy-2-nonenal

ACC - acetyl-CoA carboxylase

ADRB - adrenergic receptor gene

AgRP - agouti-related peptide

AMPK - AMP-activated protein kinase

ANT - adenine nucleotide translocase

ARC - arcuate nucleus

ATP - adenosine triphosphate

BAT - brown adipose tissue

BBB - brain blood barrier

BCA - bicinchoninic acid assay

BDNF – brain-derived neurotrophic factor

BIA - bioelectrical impedance analyses

BMI - body mass index

BMR - basal metabolic rate

CNS - central nervous system

DAPI - 4',6-diamidino-2-phenylindole

DCF - dichlorofluorescein

DCFH-DA - 2',7'-dichlorfluorescein-diacetate

DMEM - Dulbecco's Modified Eagle's medium

ECAR - extracellular acidification rate

ECL - enhanced chemiluminescent

ETC - electron transport chain

ETF - electron transfer flavoprotein

$FADH_2$ - flavin adenine dinucleotide

FCCP - carbonyl cyanide p-trifluoro methoxyphenylhydrazone

FTO - fat mass and obese associated

GPx - glutathione peroxidase

GSH - glutathione

GWAS - genome wide association study

HRP - horseradish peroxidase

IASO/IOTF – International Association for the Study of Obesity/The International Obesity Task Force

IMS - intermembrane space

LEP - leptin

LEPR - leptin receptor

MC4R - melanocortin 4 receptor

MHC - myosin heavy chain

MIM - mitochondrial inner membrane

mt-cpYFP - mitochondrial-targeted circularly permuted yellow fluorescent protein

NADH - nicotinamide adenine dinucleotide

NEAT - non-exercise activity thermogenesis

NPY - neuropeptide Y

OCR - oxygen consumption rate

ODR - obese diet resistant

ODS - obese diet sensitive

PBS - phosphate buffered saline

PET-CT - positron-emission tomography and computed tomography

POMC - pro-opiomelanocortin

PRx - peroxiredoxin

PTP - permeability transition pore

PUFA - polyunsaturated fatty acids

PYY - peptide YY

ROS - reactive oxygen species

SDH - succinate dehydrogenase

SH2B1 - SH2B adaptor protein 1

SIRT1 - silent mating type information regulation 2 homolog 1

SMR - standard metabolic rate

SOD - superoxide dismutase

T2DM - type 2 diabetes mellitus

TCA - tricarboxylic acid

TMRE - tetramethylrhodamine, ethyl ester

UCP - uncoupling protein

WHO - The World Health Organization

α-MSH - α-melanocyte stimulating hormone

LIST OF FIGURES

LIST OF TABLES

CHAPTER ONE - GENERAL INTRODUCTION

OBESITY

—*DEFINITION*

The World Health Organization (WHO) defines obesity as an "abnormal or excessive fat accumulation that may impair health" (Obesity and Overweight Fact Sheet N°311 Updated March 2011). Both obesity and the degree to which one is overweight are commonly assessed by using the body mass index (BMI), which is defined as a person's weight in kilograms divided by the square of the person's height in meters (kg/m^2). For most people, BMI is a reliable indicator of whole body fat. An adult individual is considered to have a healthy weight with a BMI of 18.5-24.9 kg/m^2; to be overweight with a BMI of 25-29.9 kg/m^2; and to be obese with a BMI of ≥ 30 kg/m^2. A child is considered overweight with a BMI-for-age between the 85^{th} percentile and the 95^{th} percentile, and obese with a BMI-for-age above the 95^{th} percentile. However, since BMI does not directly measure body fat, some people such as very muscular athletes may have a BMI above 30 even though they do not have excess body fat. Therefore, other methods of measurement of body fat and body fat distribution are sometimes used, such as waist circumference (marker of visceral obesity), waist-to-hip circumference ratio (distribution of fat), and bioelectrical impedance analysis (BIA) (total fat mass).

—*THE WORLDWIDE EXTENT OF OBESITY*

The International Obesity Task Force (IASO/IOTF) analysis in 2010 estimated that worldwide, approximately 1 billion adults are currently overweight (BMI 25-29.9 kg/m²), and that a further 475 million are obese (BMI > 30 kg/m²). The growing prevalence of childhood obesity is also a major concern. Globally, up to 200 million school-aged children are estimated to be either overweight or obese; of those, more than 40 million are obese. It is estimated using the data from IASO/IOTF that by the year 2025, levels of obesity could be as high as 45-50% in the USA, between 30-40% in Australia and England, and over 20% in Brazil.

—*OTHER DISEASES ASSOCIATED WITH OBESITY*

The WHO reports that overweight and obesity are the fifth leading risk factors for adult death globally. Obesity is associated with cardiovascular disease, type 2 diabetes mellitus (T2DM), certain forms of cancers and sleep-breathing disorders (Kopelman *et al.* 2000). In addition, globally, overweight and obesity may cause 44% of the diabetes burden, 23% of the ischemic heart disease burden and between 7% and 41% of certain cancer burdens. As a result, it is estimated that at least 2.8 million adults worldwide die each year from diseases associated with being overweight or obese (Obesity and Overweight Fact Sheet N°311 Updated March 2011).

—*WHAT CAUSES OBESITY AND OVERWEIGHT?*

The fundamental cause of obesity and overweight is an imbalance between energy intake and energy expenditure. Such an imbalance is primarily due to an increased intake of energy-dense diets and a decrease in physical activity. It is also interesting to consider the idea that some people are more biologically susceptible to the development of obesity than others. As early as 1962, Neel introduced the "thrifty genotype" hypothesis, in which he defined the "thrifty genotype" as "being exceptionally efficient in the intake and/or utilization of food" (Neel *et al.* 1962). During the history of human development, evolution occurred steadily and gradually over millions of years. Since humans existed as hunter-gatherers who suffered severe episodes of feast and famine, individuals with the "thrifty genotype" might have more chance to survive than those without "a thrifty genotype". Therefore, the human genome evolved and particular traits were selected under such a hunter-gatherer environment. However, over the past 100 years, there has been a remarkable change in modern society, characterized generally by food abundance and a sedentary lifestyle, which directly results in energy surplus and less physical activity, respectively. Ironically, those "thrifty genes" that evolved for selective advantage and survival are now being exposed as disadvantageous in a sedentary environment. Therefore, the combination of "thrifty genes", food abundance, and sedentary lifestyle results in a disharmony of gene-environment interaction, leading to a "threshold" of biological significance, manifested as several modern chronic diseases such as obesity, T2DM and cardiovascular diseases.

Current treatments for obesity are aimed at reducing energy intake or increasing energy expenditure or having an effect on both. Strategies include behavioral alteration (reduction in diet and increase in physical exercise), and medical or surgical treatments. However, one to two thirds of obese patients fail to maintain weight loss over the long term on dietary and/or exercise programs (Mann *et al.* 2007). Over the years, only three types of drugs have been available for the treatment of obesity in the United States: Sibutramine, Orlistat, and Rimonabant. They exert their effects on decreasing energy intake either by acting on satiety centers in the brain or by reducing the absorption of dietary energy or by increasing metabolic rate (Harper *et al.* 2008). However, due to safety concerns, only one drug is currently available in North America for the treatment of obesity. This is Orlistat (Xenical), which decreases the absorption of fat. Therefore, there is a great need for new therapeutic approaches.

FACTORS CONTROLLING ENERGY INTAKE

—*HORMONES & CENTRAL NERVOUS SYSTEM*

Over the past decade, there has been great progress in understanding the physiological systems that regulate energy intake. For example, leptin and insulin have been linked to long-term feeding behavior whereas ghrelin and peptide YY (*PYY*) have been shown to regulate short-term feeding behavior (Marx *et al.* 2003). In addition, researchers also have found that certain brain regions such as the arcuate nucleus (*ARC*) play a critical role in regulating these hormones that exert their effects on whole body energy metabolism (Lenz

et al. 2008). The ARC is located in the hypothalamus and it includes two major types of neurons with opposing effects. One type of neuron secretes peptide neurotransmitters called agouti-related peptide (*AgRP*) and neuropeptide Y (*NPY*), both of which stimulate appetite and decrease metabolism. Whereas, the other type referred to as POMC/CART neurons, suppresses appetite by secreting α-melanocyte stimulating hormone (*α-MSH*) (Lenz *et al.* 2008).

Leptin is released from adipocytes and transported across the brain blood barrier (BBB) into the central nervous system (CNS) (Marx *et al.* 2003). There, leptin stimulates POMC/CART neurons and inhibits AgRP/NPY neurons by binding leptin receptors, which are highly expressed in the ARC. Blood leptin levels are directly correlated to adiposity levels. Decreased leptin levels from declining fat stores leads to the activation of AgRP/NPY neurons and the inhibition of POMC/CART neurons, subsequently resulting in the stimulation of appetite. Insulin exerts the same effect as leptin but to a lesser extent. In the fasting state or immediately before meals, ghrelin levels rise and stimulate appetite by the activation of AgRP/NPY neurons through the ARC. By contrast, PYY plays an important role in satiety by acting in the ARC and inhibiting AgRP/NPY neurons and activating POMC/CART neurons (Table 1.1). Other hormones act via the CNS and include adiponectin and visfatin, which are derived from adipocytes, as well as obestatin, cholecystokinin and glucogan-like peptide-1, which are secreted from cells in the gastrointestinal tract (Lenz *et al.* 2008). In summary, the neurohormonal control of short-term and long-term energy intake is mediated by hormones, secreted from peripheral tissues, which interact with two general types of neurons (orexigenic and anorexigenic) in the ARC.

TABLE 1.1 Overview of the major hormones associated with energy intake

Hormone	Primary sites of synthesis	Role in CNS	Major functions	References
Leptin	Adipocytes	+ POMC/CART - AgRP/NPY	- food intake + energy expenditure + muscle glucose uptake + liver glucose production	Friedman 1993 Halaas 1995 Gautron 2011
Insulin	Pancreatic beta-cells	+ POMC/CART - AgRP/NPY	- food intake + muscle glucose uptake + fat cell glucose uptake	Woods 1979 Kahn 2000 Schwartz 2002
Grelin	A-cells of gastric fundus	+ AgRP/NPY	+ food intake + gastric motility	Kojima 1999 Tschöp 2000 Briggs 2011
PYY	L-cells of distal small and large intestine	+ POMC/CART - AgRP/NPY	- food intake - gut motility - pancreatic secretion	Adrian 1985 Batterham 2002 Gardiner 2008

+ Activate; - Inhibit

—*GENETIC FACTORS AFFECTING ENERGY INTAKE*

As reviewed by Farooqi and O'Rahilly, several genes that are involved in monogenic forms of human obesity have been identified. These include leptin (*LEP*), leptin receptor (*LEPR*), pro-opiomelanocortin (*POMC*), and melanocortin 4 receptor (*MC4R*) (Farooqi and O'Rahilly 2004). The frequency of these monogenic diseases is very rare, but elucidating their molecular mechanisms is important for improving our understanding of the more common forms of human obesity. Bouchard and colleagues conducted a seminal study that clearly demonstrated the importance of genetic factors in determining the susceptibility to gaining weight in response to diet (Bouchard *et al.* 1990). In this study, 12 pairs of healthy monozygotic twins were submitted to a 1000 kcal energy surplus 6 days/week for 100 days. There was a significant inter-individual difference in the adaptation to over-feeding. However, there was more variance (over 3 times) in the response between pairs than within pairs for the changes in body weight. The authors explained that such variability in response to diet could result either from individual variation of energy storage or from variation of energy expenditure during rest. These findings led to the overall conclusion that genetic factors play a significant role in response to diet and energy balance.

Obesity is now considered to be a polygenic disease, and as such, it is a challenge to perform well-controlled studies to identify the contribution of specific genes in the development of obesity. One of the most powerful tools for revealing genes associated with human obesity are the genome wide association studies (GWAS). So far, GWAS of genetic variants have identified approximately 30 loci that influence BMI and the risk of

obesity (Feero *et al.* 2010). The most significant studies identified the gene *FTO* (fat mass and obese associated), showing that genetic variation in *FTO* is reproducibly associated with increased BMI among more than 38,000 participants from 13 cohorts (Frayling *et al.* 2007). Other loci detected in GWAS include *MC4R*, brain-derived neurotrophic factor gene (*BDNF*) and SH2B adaptor protein 1 gene (*SH2B1*) (Willer *et al.* 2009, Thorleifsson *et al.* 2009).

Most of the genes identified to date are expressed in the CNS, which is generally consistent with the idea that genetic factors play a crucial role in the regulation of energy intake. However, currently identified loci that contribute to obesity are characterized by small effect sizes, suggesting that more genes need to be uncovered in the future (Bouchard *et al.* 2010). Therefore, it is possible that hundreds of genes, each with small effects, interact with each other and exert an obese phenotype (Hebebrand *et al.* 2010).

FACTORS CONTROLLING ENERGY EXPENDITURE

—*WHOLE BODY ENERGY EXPENDITURE*

Energy expenditure can be categorized into obligatory thermogenic or facultative thermogenic processes (Stock *et al.* 1999). This is summarized in Table 1.2. Obligatory thermogenesis is the energy used for all the essential cellular and organ functions such as maintenance of ion gradients across cell membranes, as well as for RNA and protein

synthesis. It also comprises special physiological functions including pregnancy, growth and lactation. Basal metabolic rate (BMR) is the major contributor to obligatory thermogenesis. BMR is defined as the amount of energy expended during a resting and unfed state, and at thermoneutrality. The thermic effect of food is the heat produced during digestion and absorption of food. Facultative thermogenesis refers to the increases in thermogenic capacity that occur in response to changes in an animal's state (e.g., exercise trained) or environment (e.g., acute exposure to cold temperature). Facultative thermogenic processes occur mainly in brown adipose tissue (BAT) and skeletal muscle, and can be further divided into five forms (Table 1.2.). Cold-induced shivering thermogenesis occurs primarily in skeletal muscle. Non-shivering thermogenesis and diet-induced thermogenesis mainly take place in BAT. These processes can be rapidly turned on and off (Argyropoulos and Harper 2002). Non-exercise activity thermogenesis (NEAT) is energy expended by movement other than exercise, e.g., that associated with daily living, maintenance of posture and fidgeting. The mechanisms that regulate NEAT are still unknown. Exercise clearly can cause substantial increases in skeletal muscle thermogenesis. *Adaptive thermogenesis* is a term that is often erroneously used to describe facultative thermogenesis. Generally, the term *facultative thermogenesis* is classical non-shivering thermogenesis (meaning that it can be turned on and off immediately) while *adaptive thermogenesis* (meaning that it needs hours or days to develop) can be induced by specific conditions such as a high fat diet, cold environmental temperature, or exercise training.

Table 1.2 Whole body energy utilization Thermogenesis (energy expenditure) is classified into two categories: obligatory thermogenesis and facultative thermogenesis. Obligatory thermogenesis refers to the heat produced by all the essential processes that maintain the body in a basal state at thermoneutral temperature. It also includes the energy used for special physiological needs, such as growth and reproduction. Facultative thermogenesis refers to the increases in thermogenic capacity that occur in response to changes in an animal's state. There are five subcategories of facultative thermogenesis. Cold exposure induces shivering thermogenesis in skeletal muscle, and non-shivering thermogenesis in BAT (and possibly also in skeletal muscle). Non-exercise activity thermogenesis (*NEAT*) is energy expended by movement other than exercise, such as daily living, maintenance of posture and fidgeting. Exercise can cause great increases in total body energy expenditure. (Adapted from Tseng 2010, and based on fundamental concepts put forth by Stock 1983).

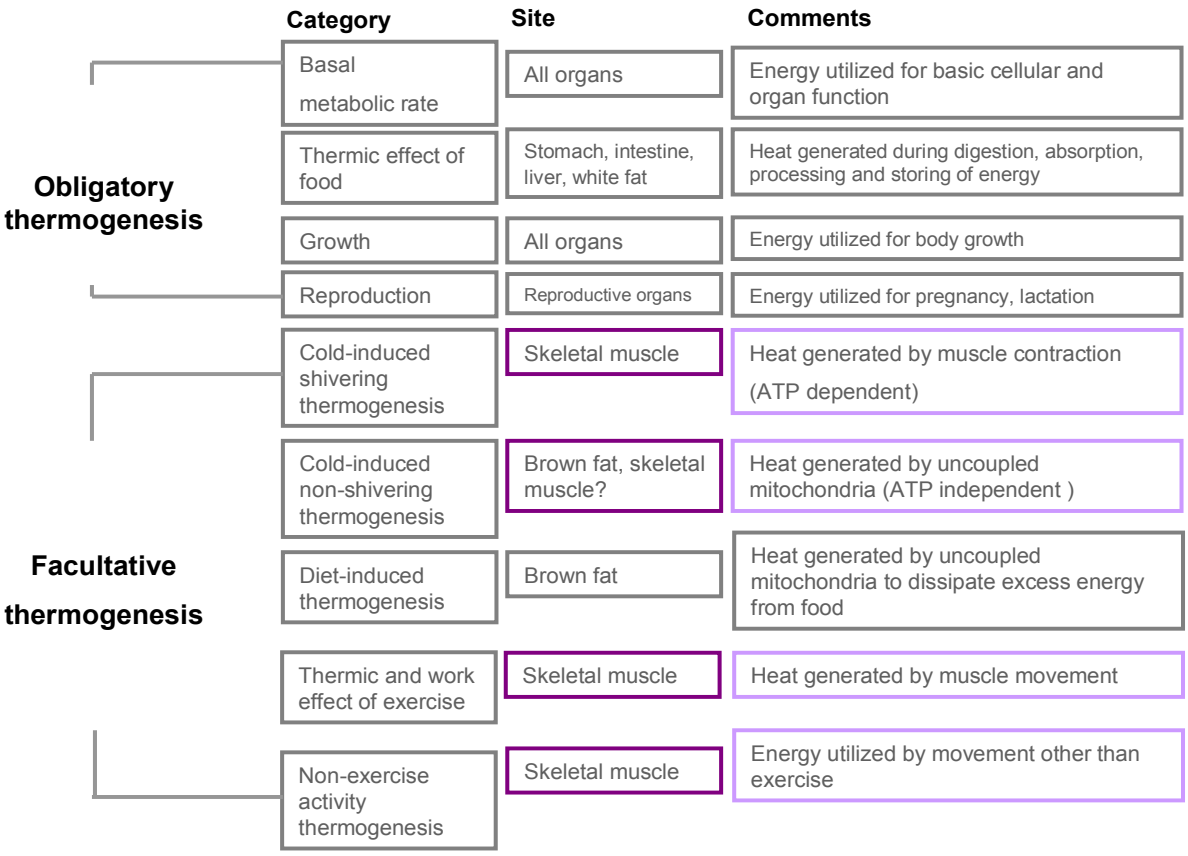
Category
Site
Comments
Obligatory thermogenesis
Basal metabolic rate
All organs
Energy utilized for basic cellular and organ function
Thermic effect of food
Stomach, intestine, liver, white fat
Heat generated during digestion, absorption, processing and storing of energy
Growth
All organs
Energy utilized for body growth
Reproduction
Reproductive organs
Energy utilized for pregnancy, lactation
Facultative thermogenesis
Cold-induced shivering thermogenesis
Skeletal muscle
Heat generated by muscle contraction (ATP dependent)
Cold-induced non-shivering thermogenesis
Brown fat, skeletal muscle?
Heat generated by uncoupled mitochondria (ATP independent)
Diet-induced thermogenesis
Brown fat
Heat generated by uncoupled mitochondria to dissipate excess energy from food
Thermic and work effect of exercise
Skeletal muscle
Heat generated by muscle movement
Non-exercise activity thermogenesis
Skeletal muscle
Energy utilized by movement other than exercise

—ENERGY EXPENDITURE ASSOCIATED WITH SPECIFIC TISSUES

Mass-specific energy requirements vary considerably between tissues. Brain, heart, skeletal muscles and BAT have high energy demands, while white adipose tissue, bone and skin have lower energy requirements. BAT is mainly responsible for cold-induced and diet-induced non-shivering thermogenesis (Stock *et al.* 1999). BAT is a highly innervated and vascularized tissue and contains large numbers of mitochondria, which possess a unique protein, uncoupling protein 1 (UCP1). UCP1 dissipates protonmotive force and uncouples respiration from the synthesis of ATP, and, consequently, the energy from the protonmotive force is released in the form of heat. Recent research has unequivocally demonstrated that healthy adult humans have significant levels of active BAT, putting to rest the longstanding controversy about the presence or absence of BAT in adult humans (Cypess *et al.* 2009*,* Van Marken *et al.* 2009, Virtanen *et al.* 2009). Previous to these findings, it was thought that BAT was only important in newborns and small mammals. However, findings demonstrated that BAT is located in the upper chest and neck of some adults. Positron-emission tomography and computed tomography (PET-CT) scans indicated that BAT activity correlates inversely with BMI (Cypess *et al.* 2009).

Skeletal muscle accounts for about 40% of adult body mass and plays an important role in exercise thermogenesis and NEAT (Clarke *et al.* 2010). Even at rest, skeletal muscle accounts for approximately 20% of resting metabolic rate (Zurlo *et al*. 1990). There is no doubt that physical exercise is the most effective way to increase energy expenditure substantially. However, many obese individuals have difficulties in exercising. Skeletal

muscle utilizes energy ultimately from dietary sources and this is largely coupled to ATP production. Nevertheless, as discussed below, uncoupled oxidative phosphorylation is also important in skeletal muscle. Physical exercise activates ATP hydrolysis for muscle contraction and increases energy expenditure. Hugh and Allan Huxley first proposed the sliding filament theory of muscle contraction in 1954 (Huxley *et al.* 1954). The theory stated that skeletal muscle contracts when two types of filaments containing the proteins myosin and actin "slide" past each other without changing the length of the filament (Huxley *et al.* 1954). Subsequent research showed that myosin contains ATPase activity and is fueled by ATP hydrolysis to generate the power stroke required to "slide" the filaments across each other by binding, rotating, and finally detaching from the actin (Szent-Györgyi 2004). It is often assumed that muscle tissue is also an important site of non-shivering thermogenesis during cold exposure even though there is no direct approach to measure it separately from other muscle thermogenic processes.

It is estimated that the brain consumes 20% of total body oxygen consumption although it only accounts for 2% of total body weight (Rolfe *et al.* 1997). In adults, the brain uses glucose as its primary metabolic substrate. During early postnatal life, the brain also uses other molecules such as free fatty acids, glycerol, and ketone bodies as fuels. In addition, lactate can also be used by the brain in adults during hypoglycemia (Dombrowski *et al.* 1989). The majority of the glucose consumed by the brain is either generated in other organs by endogenous glycogenolysis and/or gluconeogenesis or is provided directly from external fuels (diet). As early as 1977, Bier *et al.* postulated that since there was a significant linear relationship between glucose production and brain weight from

premature infants through to adulthood, the brain must utilize the majority of the glucose produced by the body (Bier *et al.* 1977). Glucose transported into the brain has to cross two distinct barriers, the blood brain barrier (BBB) and the plasma membranes of nerve cells. In humans, the predominant cerebral glucose transporters are GLUT1 and GLUT3. The former is a glucose carrier of gray matter astrocytes, while the latter is the major transporter in nerve cells (Morgello *et al.* 1995). Both *in vitro* and *in vivo* studies have shown that Na^+-K^+-ATPase activity increases significantly during postnatal development until adulthood, and such increases in activity coincide with the development of mitochondria and increased of oxidative metabolism, indicating that the transmission of the nerve impulses and the maintenance of cellular membrane potential are the major energy consuming processes in the brain (Erecinska *et al.* 2004).

The liver contributes to about 17% of total body oxygen consumption, even though it only accounts for 2% total body weight (Rolfe *et al.* 1997). The liver plays an important role in three major metabolic processes: fuel cycles, protein synthesis and degradation, and urea synthesis. Fuel cycles account for 18-30% of total cellular oxygen consumption in hepatocytes (Rabkin and Blum 1985). The degree of flux through fuel cycles is not constant, and changes depending on physiological states. For example, cycling glucose/glucose 6-phosphate decreased in the liver of starved rats compared to fed rats (Bontemps *et al.* 1978, Katz *et al.* 1978). The energy cost of protein synthesis has been estimated to account for 27% of total cellular ATP, while the energy cost of protein degradation is estimated to cost 3% of total cellular ATP in the liver (Reeds *et al.* 1987, Gill *et al.* 1989). Another major energy demanding process in the liver is urea synthesis. Assuming that the synthesis of one

molecule of urea costs four molecules of ATP, ureagenesis in rat liver accounts for 8-12% of total hepatic ATP use (Summers *et al.* 1988). Other tissues with high energy demands include the heart and kidneys. It is estimated that they account for about 17% of total body oxygen consumption even though they only account for less than 1% of total body weight (Rolfe *et al.* 1997).

—*GENETIC FACTORS AFFECTING ENERGY EXPENDITURE*

The role of energy expenditure in the development of human obesity is much less clear than the role of energy intake. Due to the genetic heterogeneity of human individuals, it is very difficult to conduct well-controlled studies of inter-individual variation in the efficiency of energy expenditure. However, studies on monozygotic twins provide strong evidence for genetic factors in different capabilities to lose weight. Bouchard *et al.* studied weight loss in 7 pairs of identical twins in response to a negative energy balance stimulated by increased physical exercise. Between-pair variation for weight loss was significantly higher than within-pair variation ($p<0.05$), indicating that exercise-induced weight loss may depend on certain genotypes; a unique combination of certain genes carried by an individual that is shared only by identical twins (Bouchard *et al.* 1994). In addition, Hainer *et al.* studied obese monozygotic twins and found a significantly higher variation (5.9 –12.4 kg) in weight and fat mass losses between pairs than within pairs in response to a very low energy diet (approximately 380 kcal/day) and increased physical exercise (Hainer *et al.* 2000). Further study showed that variation in weight loss could be caused by differences in metabolic

efficiency, which is defined as the energy intake per unit of body mass or body surface area necessary to maintain body weight (Hainer *et al.* 2001). Levine and colleagues showed that there was a 10-fold difference in fat storage among subjects responding to overfeeding (1000 kcal/day surplus). These differences in fat storage were found to be derived from differences in their increased total energy expenditure, mainly attributed to differences in NEAT (Levine *et al.* 1999). Physiological studies observed that changes in energy balance modulate NEAT; NEAT increases with overfeeding while decreases with underfeeding (Levine *et al.* 2002). However, very little evidence is available to study the physiological regulation of NEAT and its components. NEAT is highly variable, and an active person can expend 2000 kcal per day more than an inactive person of similar size (Levine *et al.* 2007). These observations suggest that the activity of NEAT may be genetically programmed. All these studies highlight the importance of energy expenditure in maintaining body weight. However, a significant limitation of these studies is the fact that muscle-associated energy expenditure was studied as a black box, disregarding the molecular or/and biochemical bases for the apparent variability.

So far, GWAS of genetic variations related to energy expenditure have produced fairly inconsistent results. Adrenergic receptor genes (*ADRB*) play an important role in adipocyte metabolism and therefore, the role of the ADRB3 Trp64Arg polymorphism has been thoroughly studied in weight loss. Carriers of Arg64 were shown to be more resistant to weight loss among homozygotes and women (Yoshida *et al.* 1995, Shiwaku *et al.* 2003), but other studies did not confirm this association (Fumeron *et al.* 1996, Rawson *et al.* 2002). However, Xinli and colleagues described increased weight loss in children carriers of Arg64

(Xinli *et al.* 2001). Studies focusing on the association between uncoupling protein 3 (UCP3) polymorphisms and obesity also yielded conflicting results. For example, one study showed that there was a statistical association and linkage between -55CT and BMI, and that subjects carrying the T allele had an average BMI 3.5% lower than those without it (Liu *et al.* 2005). Another study observed that females who carry the UCP3 gene -55CT polymorphism had higher waist-to-hip ratio than those without it, but there were no significant differences of BMI between the two groups (Cassell *et al.* 2000). On the contrary, another group found no association of this allele with obesity (Dalgaard *et al.* 2001). However, many studies of the polymorphisms of A-3826G, A-1766G, A-112C and Ala64Thr in the UCP1 gene have been identified to be associated with obesity, T2DM and lipid-related diseases (Jia *et al.* 2010). One thing that is clear from such studies is that obesity is a complex disorder that involves many genetic, environmental and behavioral factors.

SKELETAL MUSCLE IN OBESITY

Clinical and non-clinical observations reveal that certain obese individuals can achieve higher weight loss in response to the same low calorie diet compared to others. At the Weight Management Clinic of the Ottawa Hospital, we have documented a 10-fold variation in the rate of weight loss in highly compliant patients on a weight loss program (minimal exercise and a 900 kcal/day meal replacement diet) (Harper *et al.* 2002). The patients who were at the highest and lowest quintiles for percent of body weight loss during the first 6 weeks of the weight loss program were defined as obese diet sensitive (ODS) and obese diet resistant (ODR), respectively. Given that rate of weight loss varies so

dramatically in individuals having similar initial body weight when energy intake is held constant (900kcal/day), it is plausible that differences of energy expenditure might be a major cause for such variable “phenotypes”.

As discussed above, skeletal muscle is a very important tissue for thermogenesis: exercise-induced thermogenesis, cold-induced shivering thermogenesis and NEAT. Also, skeletal muscle is a major determinant of whole body resting energy expenditure (approximately 20%), mainly due to the fact that it accounts for, on average, about 40% of adult body weight. Given the quantitative importance of muscle to whole body energy expenditure, it is theoretically possible that variation in skeletal muscle energy efficiency could contribute to the variation of weight loss. The characteristics of skeletal muscle that our laboratory has studied in relation to rate of weight loss include gene expression, fiber type, mitochondrial proton leak rate and cellular ROS levels (discussed in detail below).

—*GENOME EXPRESSION ANALYSES*

Several research groups carried out transcriptomic studies to identify changes in skeletal muscle gene expression in response to weight loss or weight gain. First, Larrouy and colleagues investigated changes of skeletal muscle gene expression in obese women who had a 4-week very low calorie diet (approximately 1000kcal/day) (Larrouy *et al.* 2008). There was an upregulation of the genes related to long-term calorie restriction while there was a downregulation of the genes related to insulin and ubiquitin-mediated proteolysis, indicating that a shift toward oxidative metabolism may be a consequence of weight loss.

Meugnier and colleagues observed changes in gene expression in skeletal muscle in lean men in response to fat overfeeding (28 days, addition of 70g of lipid to the usual daily diet) (Meugnier *et al.* 2007). The main pathways that were inhibited by overfeeding included fatty acid oxidation and lipolysis. Moreover, Sparks and colleagues showed downregulation of the genes involved in mitochondrial oxidative phosphorylation in skeletal muscle of healthy individuals in response to a 35% fat diet for 3 days (Sparks *et al.* 2005).

The expression of genes in *rectus femoris* biopsies has been analyzed in previous studies of ODS and ODR patients (Gerrits *et al.* 2010). There was a significant upregulation of gene relevant to mitochondrial oxidative phosphorylation, cell cycle, and protein turnover sets in ODS compared to ODR patients. Results were validated by further analyzing gene expression in *vastus lateralis* biopsies of another seven matched pairs of ODS and ODR patients. The genes with the largest differences in expression levels in ODS compared to ODR patients included *PPAR*δ (P=0.01) and *SLC25A3* (P=0.0009). *PPAR*δ is widely distributed in skeletal muscle, promotes biogenesis of mitochondria and improves oxidative characteristics (Schuler *et al.* 2006, Spiegelman 1998). The *SLC25A3* gene encodes a phosphate carrier protein that catalyzes the co-transport of phosphate and a proton into the mitochondrial matrix. In addition, whole blood gene expression prior to weight loss in ODS and ODR patients was also analyzed (Ghosh *et al.* 2011). The results showed that the protein-ubiquitination pathway (protein turnover) and the oxidative phosphorylation pathway were the most significantly upregulated pathways in ODS compared to ODR patients. Altogether these previous results showed a significant correlation of muscle gene

expression with weight loss, again consistent with the idea that skeletal muscle processes are important factor to weight loss success.

—*MUSCLE FIBER TYPE*

In humans, muscle fibers are distinguished overall as slow twitch fibers (type I) and fast twitch fibers (type II). Type II fibers can be further subdivided into fast oxidative fibers (type IIA) and fast glycolytic fibers (type IIB) (Brooke *et al.* 1970). Type I fibers have high mitochondrial content, high oxidative capacity and are more fatigue-resistant than type IIB fibers, which contain fewer mitochondria and more glycolytic enzymes. Type IIA fibers have an intermediate density of mitochondria and have both oxidative and glycolytic properties. So far, the most effective way to identify muscle fiber types relies on the expression levels of myosin heavy chain (MHC) isoforms. To date, a total of 11 MHC isoforms have been identified including slow MHC ($MHCI_{\alpha}$, $MHCI_{a}$, $MHCI_{\beta}$ and $MHCI_{ton}$) and fast MHC ($MHCII_{a}$, $MHCII_{d}$, $MHCII_{b,}$ MHC_{eom} and $MHCII_{m}$), embryonic (MHC_{emb}) and neonatal fiber (MHC_{neo}) (Pette and Staron 1999). In small rodents, pure fiber types exist: one slow type ($MHCI_{\beta}$), and three fast types including type IIA ($MHCII_{a}$), type IIX ($MHCII_{x}$) and type IIB ($MHCII_{b}$) (Pette and Staron 1999). $MHCII_{x}$ has an intermediate contractile speed between $MHCII_{a}$ and $MHCII_{b}$ (Holmes *et al.* 1999). Based on intensive analysis including DNA examination, what was originally identified in humans as type IIB is actually homologous to type IIX of small rodents. Therefore, what has been called type IIB in humans is actually type IIX, and humans do not express the fastest MHC isoform ($MHCII_{b}$). Interestingly, there is a certain population of fibers that are hybrid fibers (Smerdu *et al.* 2008). Early studies in humans

focused on the muscle fiber composition of athletes from different sports, revealing that endurance athletes have relatively more type I than type II fibers (Costill *et al.* 1976; Fink *et al.* 1977; Saltin *et al.* 1977) compared to sprinters who have more type II fibers (Costill *et al.* 1976). It is generally accepted that endurance exercise promotes the transformation of type IIB to type IIA, whereas detraining has been shown to induce the shift from type I to type II fibers (Schantz *et al.* 1987, Pette *et al.* 1997). However, studies on monozygotic twins showed that muscle fiber type is largely genetically determined (Simoneau *et al.* 1995).

Additional studies have focused on the relationship between muscle fiber type and diseases. Insulin resistance was shown to be associated with reduced proportions of type I fibers and increased proportions of type II fibers (Lillioja *et al.* 1987). Subsequent studies demonstrated increased glycolytic and reduced oxidative enzyme activities in severely insulin resistant diabetic subjects (Simoneau *et al.* 1997). Tanner and colleagues have shown that obese women possessed a lower percentage of type I muscle fibers and a higher relative percentage of type IIB fibers (actually should be IIX) than lean controls (Tanner *et al.* 2002). However, it is yet unknown whether a certain phenotype of muscle is developed during the pathogenesis of obesity/diabetes or whether it is a primary defect.

In previous studies of ODS and ODR patients, muscle fiber typing was analyzed from *vastus lateralis* biopsies of six matched pairs of ODS and ODR patients (Gerrits *et al.* 2010). Patients were in a weight stable state and there were no differences in physical activity levels between these two groups. The proportion of type I oxidative fibers was 52% higher

in ODS compared to ODR patients. In addition, type I oxidative fibers were significantly decreased in ODR compared with the lean control subjects, indicating that decreased type I oxidative fibers in ODR patients may be an important factor for weight loss failure.

—*MITOCHONDRIAL FUNCTION*

1-MITOCHONDRIAL BIOENERGETICS

Mitochondria are referred to as the 'powerhouses of cells' where energy substrates are oxidized in a stepwise series of reactions including glycolysis, fatty acid oxidation, the tricarboxylic acid (TCA) cycle and the electron transport chain (ETC). In these reactions, oxygen is the ultimate electron acceptor in the production of adenosine triphosphate (ATP). In the TCA cycle, acetyl-CoA (mainly from fatty acid oxidation and glycolysis) is progressively oxidized yielding carbon dioxide, as well as reduced forms of nicotinamide adenine dinucleotide (NADH) and flavin adenine dinucleotide ($FADH_2$), both of which then deliver their electrons to the ETC. The mitochondrial ETC is a series of protein complexes within the inner membrane of the mitochondria. The ETC draws protons from mitochondrial matrix and deposits them in the inter-membrane space (IMS), setting up a proton gradient. The potential energy of this gradient is used by F_OF_1-ATP synthase, which converts the protonmotive force into chemical bond energy stored as ATP. This overall process is referred to as oxidative phosphorylation. When protons return to the matrix exclusively through ATP synthase, the system is referred as "coupled". However, the coupling of respiration to ATP synthesis is not 100% efficient. During uncoupled oxidative

phosphorylation, the protons that are pumped out to the IMS return to the matrix through alternative leak pathways rather than through ATP synthase and therefore no ATP is produced. This is referred to as "uncoupled" oxidative phosphorylation (Figure 1.1).

2-MITOCHONDRIAL PROTON LEAK

Mitochondrial proton leak was first observed by measuring the state 4 respiration rate of isolated mitochondria from the liver when ATP synthesis was inhibited. It is present in mitochondria isolated from other major oxygen consumption tissues such as kidney, brain, and skeletal muscles of the rat (Rolfe *et al.* 1994). In early work, it was believed that proton leak was an experimental artifact of damaged mitochondria rather than a physiological process. However, Nobes and colleagues proved that mitochondrial proton leak in intact cells was similar to that in isolated mitochondria by measuring mitochondrial membrane potential at different rates of oxygen consumption in hepatocytes (Nobes et al. 1990). In addition, Rolfe *et al.* showed that mitochondrial proton leak remains significant even when ATP turnover is increased (Rolfe *et al.* 1999).

It has been estimated that mitochondrial proton leak accounts for 25% of the energy budget from isolated liver cells and about 50% of the resting respiration rate in skeletal muscle of the rat (Nobes *et al.* 1990, Rolfe *et al.* 1996). Even at a higher metabolic rate, mitochondrial proton leak still consumes approximately 35% of overall energy expenditure in muscle (Rolfe *et al.* 1999). At the whole body level, it has been calculated that mitochondrial proton leak accounts for about 20% of rat standard metabolic rate (SMR);

truly an energy-wasting process (Rolfe *et al.* 1999). Moreover, mitochondrial proton leak has been identified also in kidney mitochondria and in cells from the thymus and brain (Porter *et al.* 1993, Rolfe *et al.* 1994, Rolfe *et al.* 1999). Remarkably, studies in different mammals showed that lower mitochondrial proton leak rates correlate with an higher body mass, consistent with the idea that mitochondrial proton leak is a significant contributor to mass-specific metabolic rate (Porter *et al.* 1993). The fact that mitochondrial proton leak is highly preserved by virtue of evolution highlights that this process must play a crucial role in cell survival. As discussed in subsequent sections, the mechanism of mitochondrial proton leak remains unknown. Many studies have been focused on the identification of the specific proteins that catalyze proton leak and the elucidation of the mechanism of these proteins that regulate proton leak.

3- THE UNCOUPLING PROTEINS

In 1985, the UCP1 gene was cloned and shown to be exclusively expressed in BAT (Bouillaud *et al.* 1985). Since then, uncoupling protein 2 (UCP2) and uncoupling protein 3 (UCP3), homologues of UCP1, were discovered across several mammalian tissues (Boss *et al.* 1997, Fleury *et al.* 1997). UCP2 mRNA is widely distributed in tissues such as lung, spleen, and brain, but in most tissues, UCP2 protein expression is at very low levels or is undetectable (Baffy *et al.* 2005). UCP3 protein is mainly expressed in skeletal muscle and BAT with some expression also in the heart (Boss *et al.* 1997).

The physiological function of UCP1 is thermogenesis; mice deficient in UCP1 are cold-intolerant and more susceptible to obesity when housed at thermoneutrality (Enerbäck *et*

al. 1997, Feldmann *et al.* 2009). UCP1 protein is activated by fatty acids and inhibited by purine nucleotides, such as ATP and ADP (Cannon et al. 1998). When UCP1 is fully activated, mitochondria in BAT are highly permeable to protons, resulting in an increase of the "futile cycle" of protons for heat production (Cannon et al. 1998). Homologues of UCP1, UCP2 and UCP3 have an approximate 59% sequence homology to UCP1, and UCP2 and UCP3 shares an approximate 72% identity in mice and humans (Ricquier *et al.* 2000). The function of UCP2 and UCP3 was originally proposed as thermogenesis, similar to the facultative thermogenesis function of UCP1 in BAT. However, unlike UCP1, it has been shown that UCP2 and UCP3 are not involved in adaptive thermogenesis. UCP2 and UCP3 differ from UCP1 in that the concentration of UCP2 and UCP3 proteins is much lower in the mitochondria compared to UCP1 (0.01% - 0.1% compared to 10% of the membrane protein) (Brand and Esteves 2005). In addition, UCP3 mRNA and protein levels increase in muscles of starved rats when thermogenesis decreases (Cadenas *et al.* 1999). However, UCP3 expression is upregulated after short-term cold exposure. Prolonged cold exposure leads to a decrease in UCP3 mRNA expression, indicating that UCP3 does not have a major role in adaptive thermogenesis (Lin *et al.* 1998). The most convincing argument rises from UCP3 knock-out mice, which have normal responses to cold exposure and normal body weight (Vidal-Puig *et al.* 2000, Gong *et al.* 2000). These observations, together with the discoveries of UCPs in ectothermic fish and plants, which do not require thermogenesis, further indicated that UCP2 and UCP3 may have different functions than UCP1 (Brand and Esteves 2005).

Figure 1.1 The mitochondrial oxidative phosphorylation system: coupled and uncoupled

The electron transport chain in the mitochondrial inner membrane (MIM) reduces oxygen to water using electrons derived from reduced substrates to pump protons from the mitochondrial matrix to the intermembrane space (IMS) in order to establish a protonmotive force. The protonmotive force is used and coupled to the synthesis of ATP. Hence, the process couples substrate oxidation to ADP phosphorylation. Basal and inducible proton conductance pathways dissipate protonmotive force without ATP synthesis, producing heat. UCPs, adenine nucleotide translocase (ANT) and phosphate carrier protein are all MIM proteins involved in the regulation of mitochondrial proton leak (adapted from Harper 2008).

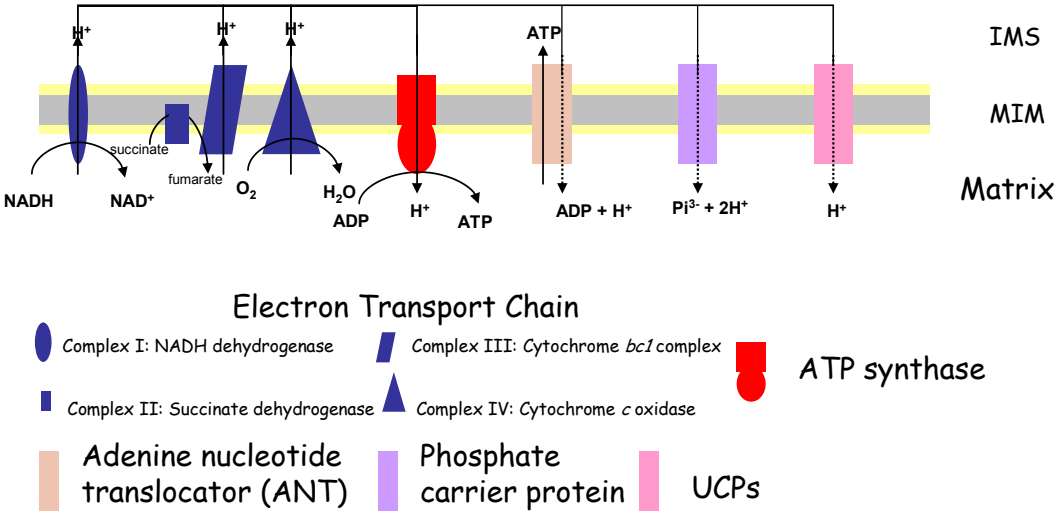
IMS
MIM
Matrix
H+
H+
H+
ATP
succinate
fumarate
NADH
NAD+
O2
H2O
ADP
H+
ATP
ADP + H+
Pi3- + 2H+
H+
Electron Transport Chain
Complex I: NADH dehydrogenase
Complex III: Cytochrome bc1 complex
ATP synthase
Complex II: Succinate dehydrogenase
Complex IV: Cytochrome c oxidase
Adenine nucleotide translocator (ANT)
Phosphate carrier protein
UCPs

4-MITOCHONDRIAL ROS

Mitochondria are the major cellular site of reactive oxygen species (ROS) production. The addition of one electron (e^-) to oxygen (O_2) forms the superoxide anion ($O_2^{\bullet -}$). Various pathways of mitochondrial ROS formation are outlined in Figure 1.2. During oxidative phosphorylation, e^- is either transferred from NADH into Complex I to coenzyme Q, or from succinate and the electron transfer flavoprotein (ETF) to coenzyme Q. Once in coenzyme Q, all e^- are transported through Complex III and cytochrome c to Complex IV, where oxygen is reduced to form water. Evidence favors Complex I and complex III as the most significant sites of superoxide generation (Sugioka *et al.* 1988, Turrens *et al.* 1980). Complex I-dependent superoxide is released solely into the matrix while superoxide from Complex III is released to both sides of the mitochondrial inner membrane (Muller *et al.* 2004). Additional free radicals include hydrogen peroxide (H_2O_2), nitric oxide ($NO^{\bullet}$), peroxyl radicals ($ROO^{\bullet}$) and the hydroxyl radical ($^{\bullet}OH$).

Various animal studies have provided strong evidence to show that increased ROS levels can cause insulin resistance (Houstis *et al.* 2006, Anderson *et al.* 2009). Lefort and colleagues have shown that mitochondria from obese individuals maintained higher ATP free energy at low metabolic flux, which may underlie the higher ROS production rate compared with lean controls (Lefort *et al.* 2010). It is generally accepted that the inflammatory environment caused by excessive nutrients in obesity and T2DM contributes to abnormal ROS production. Overload of nutrients can lead to a surplus of NADH and $FADH_2$, which accelerate flux through the mitochondrial ETC and increase ROS generation.

Figure 1.2 Generation and metabolism of reactive oxygen species (ROS). Complex I (NADH dehydrogenase) and complex III (Cytochrome bc1 complex) are the most significant sites of superoxide generation. Superoxide is converted by superoxide dismutase (SOD) to H_2O_2, which, in turn, is reduced to H_2O by catalase, glutathione peroxidases (GPx), and peroxiredoxins (Prx). TRX (ox): oxidized thioredoxin TRX (red): reduced thioredoxin (adapted from Fukai *et al.* 2011).

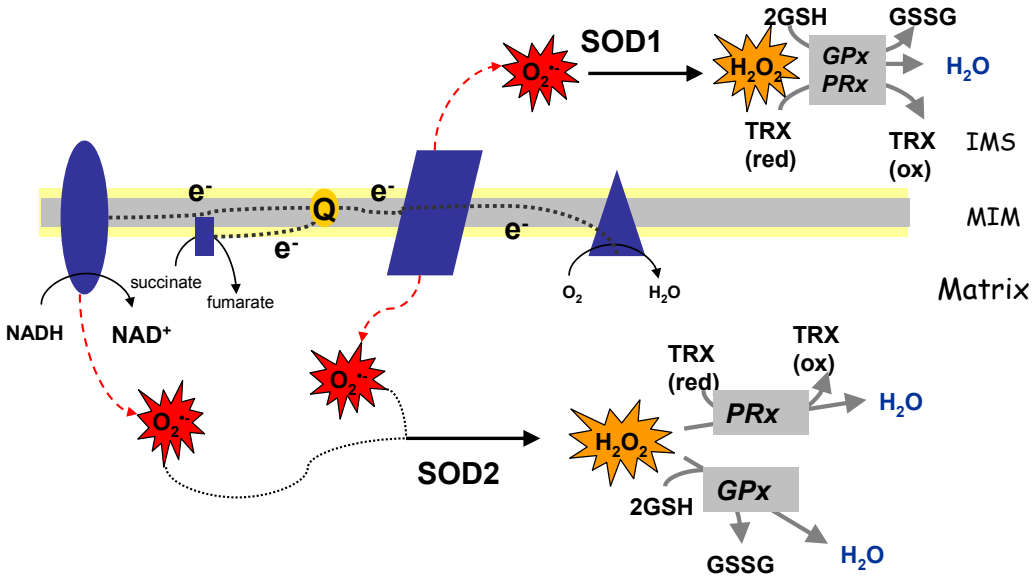

Complex I: NADH dehydrogenase

Complex II: Succinate dehydrogenase

Complex III: Cytochrome *bc1* complex

Complex IV: Cytochrome *c* oxidase

Consistent with this explanation, high-fat diets can induce mitochondrial ROS emission in both rodents and humans (Anderson *et al.* 2009).

Under normal cellular conditions, mitochondrial ROS play an important role in the modulation of numerous cell functions. However, uncontrolled mitochondrial ROS production is associated with cell injury or death. The chief enzyme involved in the dismutation of $O_2^{\bullet-}$ to H_2O_2 is superoxide dismutase (SOD). There are three isoforms of SOD in mammals: the cytoplasmic Cu/Zn SOD (SOD1), the mitochondrial MnSOD (SOD2), and the extracellular Cu/Zn SOD (SOD3). SOD1 knock-out mice showed extensive oxidative damage in the cytoplasm, while SOD2 knock-out mice have a lethal phenotype (Elchuri *et al*. 2005, Li *et al*. 1995). After the dismutation of $O_2^{\bullet-}$ to H_2O_2, the H_2O_2 is able to oxidize thiol residues on proteins and low molecular thiolating agents such as glutathione (GSH). H_2O_2 is more stable than ($O_2^{\bullet-}$), and can still damage cells by generating hydroxyl radicals through Fenton or Haber-Weiss reactions if present at high levels (Pierre *et al.* 1999). In order to prevent the generation of hydroxyl radicals, H_2O_2 can be reduced to H_2O by glutathione peroxidases (GPx), and/or peroxiredoxins (PRx).

The physiological roles of UCP2 and UCP3 are now thought to involve the attenuation of mitochondrial ROS production and thus function in the contexts of ROS signaling and protection against oxidative damage. The first evidence of this was gathered by Nègre-Salvayre and colleagues who showed that inhibition of UCP2 by GDP increased mitochondrial ROS production from rat hepatocytes (Nègre-Salvayre *et al.* 1997). Moreover, UCP2 knock-out mice were found to be resistant to infection by the intracellular

parasite *Toxoplasma gondii* through a mechanism proposed to involve higher levels of ROS produced in macrophages (Arsenijevic *et al.* 2000). In addition, Echtay and colleagues have shown that activation of mild uncoupling through UCP2 and UCP3 decreases protonmotive force, resulting in lower ROS levels and protection against ROS-related cellular damage (Echtay *et al.* 2002).

Other studies have shown that inducible proton leak through UCP2 and UCP3 needs specific activators (Brand *et al.* 2005). Echtay and colleagues showed that ROS by-product 4-hydroxy-2-nonenal (4-HNE) is required for the activation of proton leak through UCP2 and UCP3 (Echtay *et al.* 2003). It was proposed that 4-HNE produced from superoxide-induced lipid peroxidation may induce UCP activity and therefore decrease mitochondrial ROS production. In addition, fatty acids such as palmitoleic acid (C16:1) and some polyunsaturated fatty acids (PUFA) have also been shown to activate UCP2 and UCP3 (Rial *et al.* 2004). However, induced mitochondrial proton leak in the presence of activators is inhibited by purine nucleotides such as ATP and GDP (Brand *et al.* 2005). Moreover, the inhibition of UCP3 by GDP in skeletal muscle mitochondria increases membrane potential and mitochondrial ROS production (Talbot *et al.* 2004). Activation of UCP2 and UCP3, at the expense of an inefficiency in ATP production (via mitochondrial proton leak), is thus thought to slightly lower the mitochondrial membrane potential and attenuate mitochondrial ROS production (Brand *et al.* 2005). Therefore, there is good evidence to show that the primary function of UCP2 and UCP3 is to reduce mitochondrial ROS production through “mild” uncoupling.

Adenine nucleotide translocase (ANT) catalyzes the exchange of mitochondrial ATP for cytosolic ADP. It is one of the most abundant proteins of the MIM, accounting for nearly 10% of total proteins in cardiac mitochondria (Klingenberg *et al.* 2008). It has been shown that adenosine monophosphate can induce proton leak by the activation of ANT and such inducible leaks are inhibited by the inhibitor carboxyatractyloside (Cadenas *et al.* 2000). In addition, Nadtochiy and colleagues have shown that changes in proton leak were due to the covalent modification of cysteine residues in ANT, and that the overproduction of ROS activates ANT (Nadtochiy *et al.* 2006). Therefore, cells are equipped with many enzymes and processes for the detoxification of ROS consistent with the overall idea that anti-oxidative defense systems are crucial to cell survival.

In our previous studies, mRNA levels of UCP3 and mitochondrial proton leak in skeletal muscle were measured *ex vivo* from *rectus femoris* biopsies of six matched ODS and ODR patients (Harper *et al.* 2002). UCP3 mRNA and nonphosphorylating (state 4) respiration were significantly higher in mitochondria from ODS compared to ODR patients. A recent paper published from our lab showed that glutathionylation/deglutathionylation regulates ROS-induced mitochondrial proton leak through UCP2 and UCP3 but not UCP1 (Mailloux et al. 2011a). Also, GRx1 was shown to covalently conjugate GSH to purified UCP3 *in vitro*, implying that the reaction of glutathionylation of UCPs can be enzymatic. Accordingly, our future studies will be focused on the mechanisms of mitochondrial proton leak and regulation of cellular oxidative stress of ODS and ODR patients.

RATIONALE AND HYPOTHESIS

In developed and developing countries worldwide there is an obesity epidemic. Obesity is a major risk factor for many diseases and the health care costs associated with their treatment are sky-rocketing. Genetic and metabolic studies have revealed that some individuals are at greater risk for the development of obesity and obesity-related diseases than others.

Previous studies conducted in the Ottawa Hospital Weight Management Clinic have shown that there were significant differences in skeletal muscle metabolism between ODS and ODR patients. These include the findings (as detailed in previous chapter) that proton leak-dependent oxygen consumption in skeletal muscle (*rectus femoris*) was approximately 50% higher in mitochondria from ODS compared to ODR patients. The proportion of oxidative fibers (type I) was also higher in ODS than ODR patients and the muscle fiber area was increased in ODS compared to ODR and lean subjects. The current study has extended previous findings by isolating primary myoblasts from *vastus lateralis* muscle biopsies of ODS and ODR patients. Primary myoblasts have been differentiated into myotubes for the identification of *in vitro* muscle metabolic characteristics between ODS and ODR groups.

HYPOTHESIS

Myotubes from the *vastus lateralis* of ODS patients maintain a higher mitochondrial proton leak compared to myotubes from ODR patients, as previously shown in freshly isolated mitochondria from *rectus femoris* muscle biopsies.

OBJECTIVES

The specific objectives of this study were:

- To examine the mitochondrial proton leak (state 4 oxygen consumption rate) in myotubes of both ODS and ODR patients

- To further elucidate the mechanism of mitochondrial proton leak in human primary myotubes

CHAPTER TWO - RESEARCH DESIGN AND METHODS

SUBJECTS

The study was approved by the Human Research Ethics Board of the Ottawa Hospital. Signed consent was obtained from all study participants. Women participating in this study had a body mass index of 30-50kg/m^2 and were patients in the Ottawa Hospital Weight Management Program. Patients undergoing this program participated in 26 weekly 3 hour meetings consisting of a 90-minute workshop for building lifestyle skills for weight management followed by a physician visit and determinations of weight, waist circumference and blood pressure. This was followed by 6 monthly meetings to round out the year. For the first 12 weeks, patients consumed a total meal replacement of 900 Kcal/day (Optifast® 900; Nestle Nutrition, Whitby, ON, Canada) divided in 4 equal meals. Patients then made a gradual transition to a 1200 - 1800 Kcal diet over the next 4 wks. This program also provides substantial clinical and educational feedback to patients on a monthly basis (Dent *et al.* 2002).

Because compliance to a hypocaloric protocol is a major cause for poor response to dietary intervention, we selected only highly compliant patients for our sub-study. Patients were excluded if they failed to complete 75% of the 26 weekly visits and/or there was inadequate lab testing done at 1st, 3rd, or 26th week of the program such as electrolytes,

blood glucose and liver enzyme levels (Dent *et al.* 2002). Patients with medical conditions or drug use possibly affecting rate of weight loss were also excluded. The latter included abnormal thyroid indices, diabetes mellitus treated with insulin or oral hypoglycemic agents, cigarette smoking, congestive heart failure, obstructive sleep apnea, active malignancy, immobility, or previous bariatric surgery (Figure 2.1). Rate of weight loss was evaluated in the first 6 weeks of the defined 900-kcal meal replacement regimen. We then selected highly compliant women who were matched for age and body mass index (n=9 per group) in the top or bottom quintiles of percent of initial weight loss in the first 6 weeks of meal replacement to participate in the study. These patients are referred to as obese diet-sensitive (ODS) and obese diet-resistant (ODR), respectively.

MUSCLE BIOPSIES

A subset of nine ODS and ODR patients matched for age and initial body weight underwent *vastus lateralis* muscle biopsy. Biopsies were conducted several months after the completion of the meal replacement program when the weights of the patients were stable for at least 4 weeks. Weight stability was defined as weight maintenance within 5% of body weight. Biopsies were carried out before 10 AM after a 12 hour fast, using the local anesthetics lidocaine and marcaine. A 100-150 mg needle biopsy of *vastus lateralis* muscle was collected using a Bergstrom needle. The muscle biopsy was then processed for primary myoblast isolation and culture.

Figure 2.1: Clinical Protocol Women with a body mass index of 30-50kg/m^2 entered the Ottawa Hospital Weight Management Program. Rate of weight loss was evaluated in the first 6 weeks of a defined 900-kcal (Optifast® 900; Nestle Nutrition, Whitby, Canada) meal replacement regime. Only highly compliant patients were selected for study. Those in the upper quintile for rate of weight loss were defined as obese diet-sensitive (ODS), while those in the lowest quintile were defined as obese diet-resistant (ODR). Muscle biopsies from the *vastus lateralis* were taken after the completion of the program when patients were in a weight stable state.

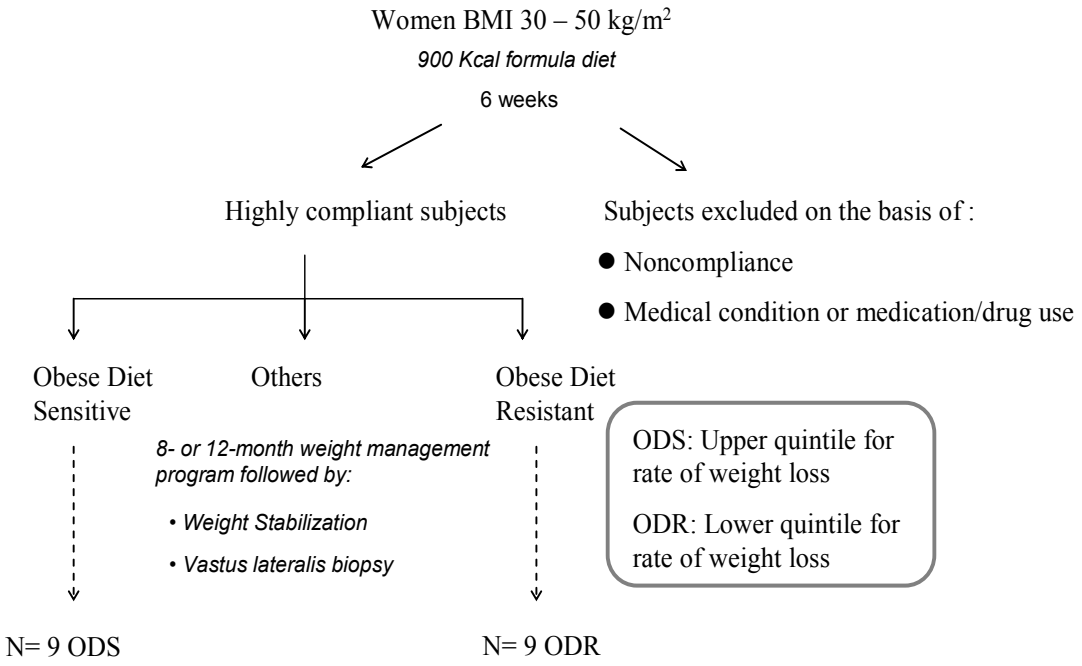
Women BMI 30 – 50 kg/m2
900 Kcal formula diet
6 weeks
Highly compliant subjects
Subjects excluded on the basis of :
Noncompliance
Medical condition or medication/drug use
Obese Diet Sensitive
Others
Obese Diet Resistant
8- or 12-month weight management program followed by:
Weight Stabilization
Vastus lateralis biopsy
ODS: Upper quintile for rate of weight loss
ODR: Lower quintile for rate of weight loss
N= 9 ODS
N= 9 ODR

Cell Culture

Muscle tissue was minced, digested with trypsin for 30 minutes and plated in growth medium consisting of Ham's F-10 media supplemented with 15% fetal bovine serum, 1% antibiotic-antimycotic, 2.5ug/mL gentamycin, 0.5mg/ml bovine serum albumin, 1umol/L dexamethazone, 10ng/mL epidermal growth factor, and 0.25pmol/L insulin. CD-56-positive primary myoblasts were immunoselected by mouse monoclonal anti-human CD-56 antibody in a MACS microbead system as previously described (Costford *et al.* 2009). Upon reaching 90% confluency, CD-56-positive primary myoblasts were induced to differentiate in low glucose (5.5 mmol/L) or high glucose (25mmol/L) Dulbecco's Modified Eagle's medium (DMEM) supplemented with 2% horse serum, 1% antibiotic-antimycotic and 2.5ug/mL gentamycin for 6 days prior to experimentation.

Desmin Immunofluorescence Staining

Desmin is a type III intermediate filament protein of skeletal muscle cells. We used immunofluorescence staining of desmin in our muscle cell cultures to evaluate the purity of primary myoblasts. 4', 6-diamidino-2-phenylindole (DAPI) was also used to visualize the nuclei. After CD-56 based immunoselection of primary myoblasts, cells were fixed with 4% paraformaldehyde in phosphate buffered saline (PBS), permeabilized with 0.5% Triton X-100 in PBS for 2 minutes and were blocked by 0.5% BSA in PBS for 10 minutes. Cells were incubated with monoclonal mouse-anti human desmin primary antibody (M0760; DakoCytomation, Glostrup, Denmark) (1:50 dilution in PBS with 0.5% BSA) for 1 hour at

room temperature, washed 3 times with PBS and then incubated with a goat-anti mouse IgG1-Texas Red secondary antibody (1:50 dilution in PBS with 0.5% BSA) and DAPI (MP01306; Invitrogen, Eugene, OR, United States) (1:250 dilution) for 1 hour at room temperature in the dark. The images of individual samples were observed by fluorescent microscopy (Axiovert 200; Zeiss, Germany), equipped with a Hamamatsu Photonics C2400 camera (Hamamatsu, Shizuoka, Japan).

Mitochondrial Metabolic Analysis

The XF24 Extracellular Flux Analyzer (Seahorse Bioscience, North Billerica, MA, United States) was employed to determine mitochondrial bioenergetics characteristics of primary myotubes (Figure 2.2-1). Primary myoblasts were seeded (50,000 cells/well) into 24-well Seahorse XF24 culture plates (28mm^2 well) with growth medium (same as cell culture growth medium). The medium was switched within one day to low or high glucose differentiation media. Myotubes were studied after 6 days of differentiation. On the day of the assay, the medium was changed to freshly prepared DMEM (plus 4mM glutamine, 1mM sodium pyruvate, 5mM or 25mM glucose, and pH 7.4). Oxygen consumption rate (OCR) was measured by monitoring the concentrations of dissolved oxygen by the XF24 Analyzer solid state sensor probes above the cell monolayer. The extracellular acidification rate (ECAR) was also assessed by the extracellular changes in pH, an indirect measurement of lactic acid production from cellular anaerobic glycolysis. To assess resting metabolic characteristics of myotubes, three measurement cycles were recorded (one measurement interval consists

Figure 2.2-1: A schematic assessment of mitochondrial bioenergetics using extracellular flux technology (XF24 Extracellular Flux Analyzer) After three baseline OCR measurements, oligomycin, FCCP and antimycin A were injected sequentially into the medium above the myotubes. The OCR measurements were recorded after each injection. ATP-linked OCR and the OCR due to proton leak is calculated using the basal and the oligomycin-insensitive rates, respectively. Injection of the uncoupling agent, FCCP, then allows the determination of the maximal respiratory capacity. Lastly, injection of the complex III inhibitor, antimycin A, allows for the measurement of non-mitochondrial oxygen consumption.

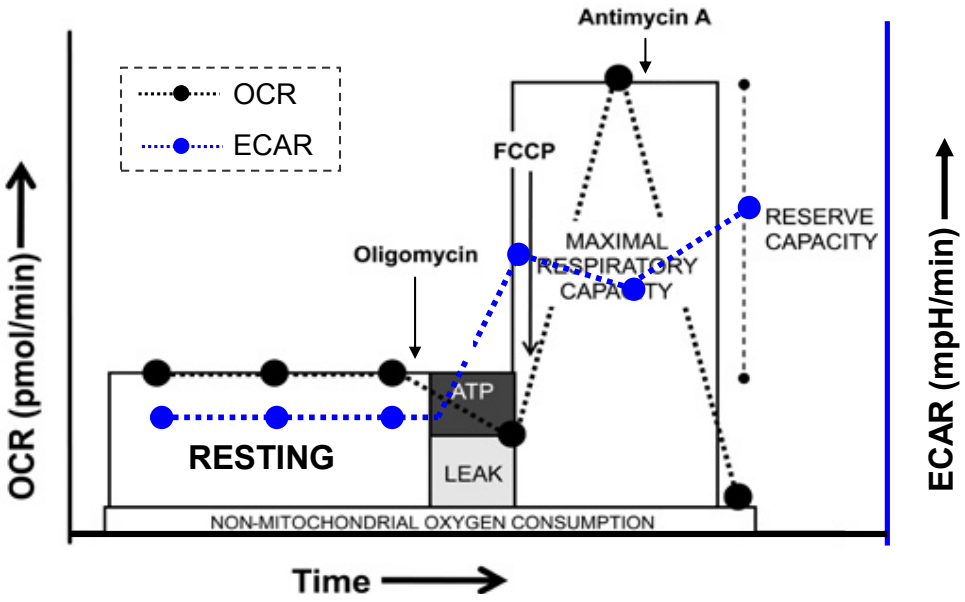
Antimycin A
OCR
ECAR
FCCP
Oligomycin
MAXIMAL
RESPIRATORY
CAPACITY
RESERVE
CAPACITY
ATP
RESTING
LEAK
NON-MITOCHONDRIAL OXYGEN CONSUMPTION
OCR (pmol/min)
ECAR (mpH/min)
Time

Figure 2.2-2: Analysis of bioenergetic pathways in mitochondria of myotubes. In the resting state, the electron transport chain (ETC) is fueled by electrons from oxidative process in cells. With the coincident pumping of protons out of the matrix, a proton gradient is established. The gradient is used by F_OF_1-ATP synthase for ATP synthesis but a small proportion of protons return to the matrix through alternative leak pathways. Leak-dependent (State 4) respiration: In this metabolic state, all protons return to the matrix through leak pathways (F_OF_1-ATP synthase is inhibited by oligomycin). Maximal respiratory capacity (FCCP-induced): In this state, mitochondria are uncoupled and the respiratory chain is functioning at its maximal rate. Non-mitochondrial oxygen consumption: After a saturating concentration of antimycin A is added, the respiratory chain is fully inhibited and the remaining oxygen consumption is extra-mitochondrial. IMS: Intermembrane space; MIM: Mitochondrial inner membrane (Figures pages 39 and 40).

Resting State

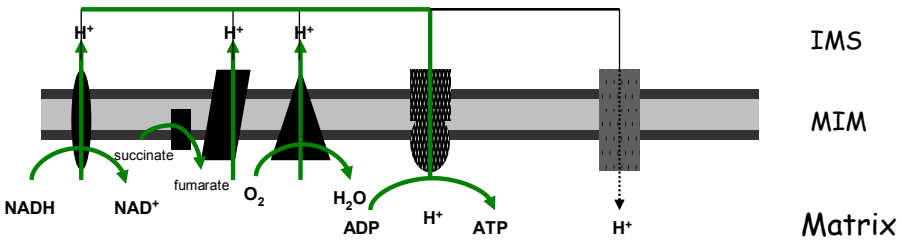

Leak-dependent (State 4) (Oligomycin)

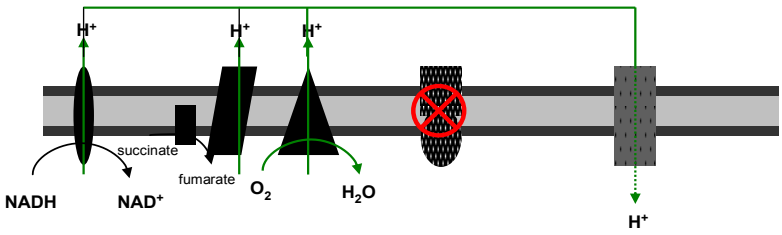

Maximal respiratory capacity (FCCP)

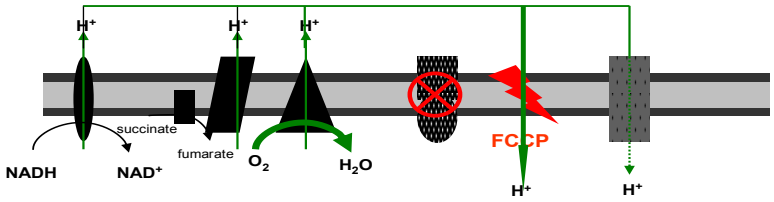

Non-mitochondrial oxygen consumption (Antimycin)

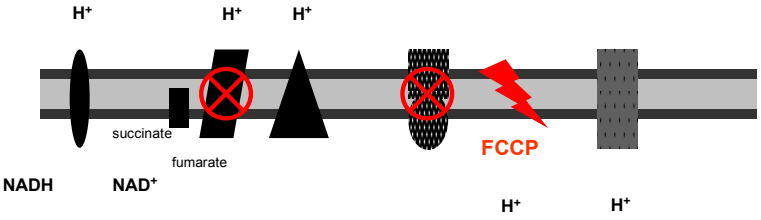

Complex I: NADH dehydrogenase

Complex II: Succinate dehydrogenase

Complex III: Cytochrome *bc1* complex

Complex IV: Cytochrome *c* oxidase

ATP synthase

Leak pathway

of 2min mixing, 2min incubation, and 2min measurement steps). To obtain leak-dependent OCR (State 4) respiration, oligomycin (500ng/mL) was injected into the wells, and three more measurement cycles followed. Mitochondrial maximal phosphorylation capacity and non-mitochondrial OCR were measured by the sequential injection of carbonyl cyanide p-trifluoro methoxyphenylhydrazone (FCCP) (1uM) and antimycin A (50nM), respectively and three measurements were recorded after each injection. OCR was normalized to total cellular protein/well. Cellular protein content was determined by the bicinchoninic acid assay (BCA assay) (Figure 2.2-2).

Mitochondrial Membrane Potential Determinations

Tetramethylrhodamine, ethyl ester (TMRE) is a lypophilic cationic dye that accumulates in the mitochondrial matrix proportional to membrane potential. TMRE is often used at high concentrations (>100nM) in self-quenching mode and therefore, mitochondrial accumulation quenches TMRE fluorescence. When membrane potential is assessed using TMRE at quenching concentrations, potential is inversely related to fluorescence levels. CD-56-positive primary myoblasts were seeded (250,000 cells/well) into 12-well plates and differentiated in LG or HG differentiation media for 6 days. Cells were incubated with TMRE (175nmol/L) (T699; Invitrogen, Eugene, OR, United States) in either LG or HG PBS with 4mM glutamine, 1mM sodium pyruvate for 10 minutes at 37°C in the dark. The TMRE-containing

Figure 2.3: Mitochondrial membrane potential determinations, using the lipophilic cationic dye, TMRE Resting State: TMRE accumulates in the mitochondrial matrix proportional to membrane potential. Mitochondrial polarization: when F_OF_1-ATP synthase is inhibited by oligomycin, mitochondrial membrane potential increases and TMRE is quenched, thus decreasing fluorescence. Mitochondrial depolarization: FCCP depolarizes the mitochondrial inner membrane, TMRE is released from mitochondria and thus TMRE fluorescence increases. (Figures pages 42 and 43)

Time = 0 **Time = 2 min.**

Resting State

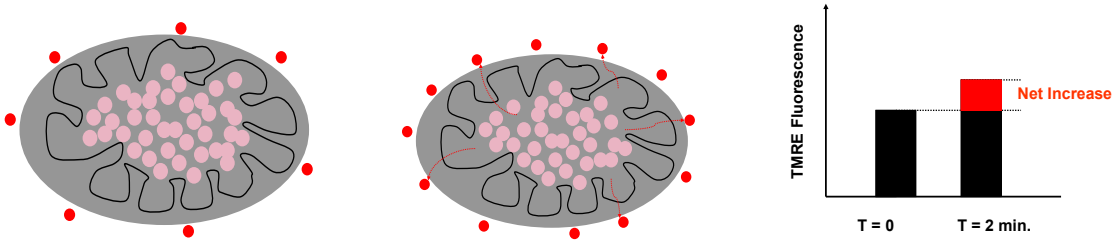

Mitochondrial inner-membrane polarization (Oligomycin)

Before Oligomycin After Oligomycin

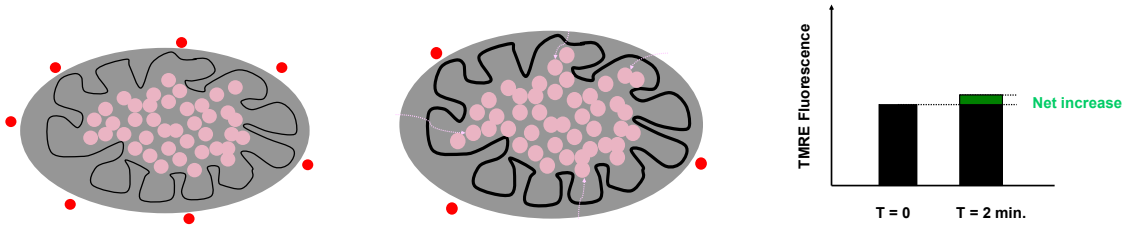

Time = 0 **Time = 2 min.**

Mitochondrial inner-membrane depolarization (FCCP)

Before FCCP After FCCP

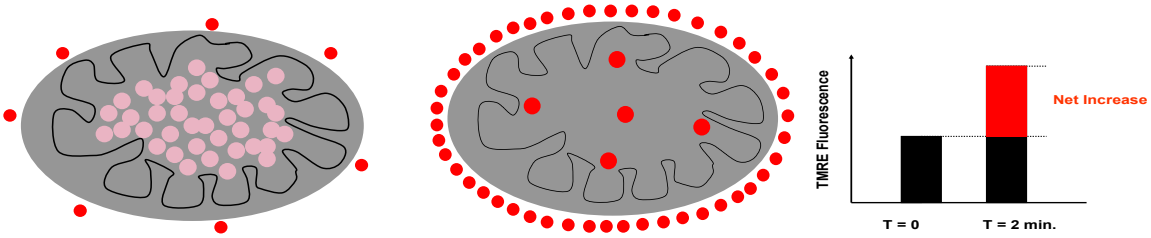

TMRE fluorescence (non-quench mode)

TMRE fluorescence (self-quench mode)

medium was removed; cells were washed in LG-PBS or HG-PBS. Fluorescence measurements (excitation 544nm, emission 590nm) were obtained by a multi-mode microplate reader (Synergy Mx, BioTek, Winooski, VT, United States) after 5 minutes of incubation at 37˚C. Then, fluorescence measurements were carried out after injecting oligomycin (50nM) and FCCP (1uM), respectively. Control wells contained no oligomycin or FCCP. The net increase of TMRE fluorescence was calculated as the value of the second measurement (T=2min) subtracted from the value of the same well in the first measurement (T=0min). FCCP was used as a positive control, since it depolarizes the mitochondrial inner membrane, releases TMRE from the mitochondrial matrix and therefore, increases dramatically the net TMRE fluorescence after its injection (Figure 2.3). The images of myotubes were also obtained using fluorescent microscopy (Axiovert S100-TV; Zeiss, Germany).

Measurement of Reactive Oxygen Species Production

After 6 days of differentiation, myotubes were washed twice with PBS and incubated with warmed (37°C) LG or HG differentiation media containing 20uM 2',7'-dichlorfluorescein-diacetate (DCFH-DA) (C400; Invitrogen, Eugene, OR, United States) for 30 min at 37°C. Cells were then washed with PBS twice and the media replaced with PBS. DCFH-DA is nonpolar and readily crosses cell membranes. Once within the cell, it is hydrolyzed by cytosolic hydrolases to DCFH. This compound reacts rapidly with hydrogen peroxide in the presence of peroxidases and (less rapidly with some other ROS) to form fluorescent

dichlorofluorescein (DCF). Absolute values were measured by a multi-mode microplate reader (excitation 488nm, emission 525nm) (Synergy Mx, BioTek, Winooski, VT, United States) and calculated by subtracting background fluorescence produced in the absence of DCFH-DA.

Intracellular ATP Concentration Measurements

ATP concentrations were measured by a StayBrite™ATP Assay Kit (Biovision Research Products; Mountain View, CA, United States) using a genetically modified variant derived from the Luciferase of *Diaphanes pectinealis* (Chinese Firefly). Myotubes were scraped in 1% Triton X-100 lysis buffer after 6 days of differentiation and then homogenized with a Dounce homogenizer. After removing cell debris by centrifugation, samples (10 µL) were added to 90µL of a reaction mix containing 10µL reaction buffer, 10µL enzyme mixture and 70µL dH_2O. The luminescence was quantified by a multi-mode microplate reader (Synergy Mx, BioTek, Winooski, VT, United States). ATP concentrations of the samples were calculated from the standard curve using linear regression. Cellular protein content was determined by the BCA assay.

Overall Mitochondrial Structure Determinations

The fluorescent marker, Mitotracker Green (MitoTracker® Green FM; Invitrogen, Eugene, OR, United States) was used to characterize overall structural aspects of mitochondrial networks in cells. Myotubes were differentiated for 6 days in LG or HG medium and

incubated with Mitotracker Green (250nM) for 30 min (37˚C). Myotubes were then washed in PBS twice after staining. The images of myotubes were obtained using fluorescent microscopy (Axiovert S100-TV; Zeiss, Germany).

Western Blotting of Key Proteins

Myotubes differentiated for 6 days in LG or HG medium were lysed in RIPA buffer (150 mM NaCl, 50mM Tris (pH 7.4), 1 mM EDTA, 1% (v/v) NP-40, 0.25% (w/v) sodium deoxycholate, protease inhibitors and phosphatase inhibitors) and protein content was determined using the BCA assay. Lysates were separated on a 12% bis-tris polyacrylamide gel and proteins were electro-transferred to a nitrocellulose membrane. Slow myosin heavy chain (sMHC) and fast myosin heavy chain (fMHC) were detected using mouse anti-slow MHC 1:1000 dilution (M8421; Sigma, St. Louis, MO, United States) and mouse anti-fast MHC 1:1000 dilution (M4276; Sigma, St. Louis, MO, United States) respectively, following by goat anti-mouse IgG conjugated with a horseradish peroxidase (HRP) 1:2000 dilution (sc2005; Santa Cruz Biotechnology, Santa Cruz, CA, United States). Complex III (core I subunit) and succinate dehydrogenase (SDH) were measured using mouse anti- Complex III 1:2000 dilution (459140; Invitrogen, Camarillo, United States) and mouse anti-SDH 1:1000 dilution (sc59687; Santa Cruz Biotechnology, Santa Cruz, CA, United States), following by goat anti-mouse IgG-HRP 1:2000 dilution (sc2005; Santa Cruz Biotechnology, Santa Cruz, CA, United States). UCP3 and tubulin (loading control) were detected using rabbit anti-UCP3 1:1000 dilution (ab-3477, ab-41038; Abcam, Cambridge, MA, United States) and mouse anti-tubulin 1:5000 dilution (T6199, Sigma, St. Louis, MO, United States), following by goat anti-

rabbit IgG-HRP (sc2030; Santa Cruz Biotechnology, Santa Cruz, CA, United States) and goat anti-mouse IgG-HRP 1:2000 dilution (sc2005; Santa Cruz Biotechnology, Santa Cruz, CA, United States). All the primary antibodies were used with 5% BSA and the secondary antibodies were used in TBST with 5% nonfat dry milk. Visualization was achieved using an enhanced chemiluminescent (ECL) substrate for HRP enzyme (Thermo Scientific, Rockford, IL, United States). Image J software was applied for the densitometry of the Western blots.

Statistical Methods

A Student's *t* test was applied to assess statistical differences between clinical parameters of ODS and ODR patients (Table 3.1, Table 3.2, Figure 3.1). The Student's *t* test was also used to access differences in MHC, Complex III, SDHA, mnSOD and UCP3 protein levels (Figure 3.2-2, Figure 3.4-2, Figure 3.5-3, Figure 3.5-4). A two-way ANOVA with a Tukey post-test was used to assess statistical differences in OCR, ECAR, mitochondrial membrane potential, ROS and ATP (Figure 3.3-1, Figure 3.3-2, Figure 3.3-3, Figure 3.5-1, Figure 3.5-2). A p value < 0.05 was used as the level of statistical significance.

CHAPTER THREE - RESULTS

STUDY SUBJECTS

Baseline parameters of the study subjects are described in Table 3.1. The results demonstrate that the biopsied patients in the ODS and ODR groups were representative of their overall cohorts of patients in the ODS and ODR quintiles. In the biopsied subjects, there were no significant differences between the two groups in terms of age, initial BMI, or initial body weight at program entry.

Characteristics of weight loss over 6 weeks of a 900 kcal diet and at the time of muscle biopsy are described in Table 3.2 for ODS and ODR groups. Again, ODS and ODR patients participating in this study were at the top and bottom quintiles for rate of weight loss, respectively. Despite similar baseline age, BMI, and weight, the mean weight loss after 6 weeks was 50.6% greater in the biopsied ODS patients than in the ODR patients ($P=0.002$). The percentage of initial body weight lost over this period was also 40.7% higher in the ODS group than in ODR group ($P=0.0003$). Body weight at the time of the muscle biopsy did not differ significantly between the two groups ($P=0.24$). In addition, percent of weight loss was significantly different between ODS and ODR patients at third week of the program until fifteenth week ($P<0.005$) (Figure 3.1).

Table 3.1: Characteristics of ODS and ODR weight loss cohorts and biopsied subgroups

	Cohort		Biopsied subjects	
	ODS	**ODR**	**ODS**	**ODR**
n	71	71	9	9
Age at program entry (years)	41(1.0)	45(2)	46(3)	51(3)
Initial BMI (kg/m^2)	37.4(0.6)	40.6(1.2)	37.7(0.9)	35.6(1.1)
Initial Weight (kg)	99.5(1.9)	109.3(3.0)	102.1(4.0)	94.2(1.8)

Data are means (SD), n=9, Student's *t* test for each parameter (NS)

Table 3.2: Weight change in biopsied groups

	ODS	ODR
Age at the biopsy (years)	48(3)	55(3)
n	9	9
Baseline at the program entry		
Weight (kg)	102.1(4.0)	94.2(1.8)
Height (cm)	164.6(1.6)	162.9(1.9)
BMI (kg/m^2)	37.7(0.9)	35.6(1.1)
6 weeks of 900 kcal diet		
Weight (kg)	90.5(3.5)	86.6(1.7)
Weight Loss (kg)	11.6(0.6)	7.7(0.4)*
% weight loss	11.4(0.2)	8.1(0.4)**
At biopsy		
Weight (kg)	89.7(5.4)	84.8(3.1)
BMI (kg/m^2)	32.9(0.5)	32.0(1.3)
BMR (kcal)	1592.8(64.5)	1514.8(36.2)
% body fat	42.1(2.2)	44.2(1.3)

Data are means (SD), n=9, Student's *t* test for each parameter

***, P<0.05**

****, P<0.001**

Figure 3.1 Rate of weight loss in ODS and ODR patients undergoing muscle biopsy. Percent weight loss for ODS (green) and ODR (red) patients is shown for the time of entry into the program (week 0), and over the subsequent 24 weeks (data from the Ottawa Hospital Weight Management Clinic) n=9

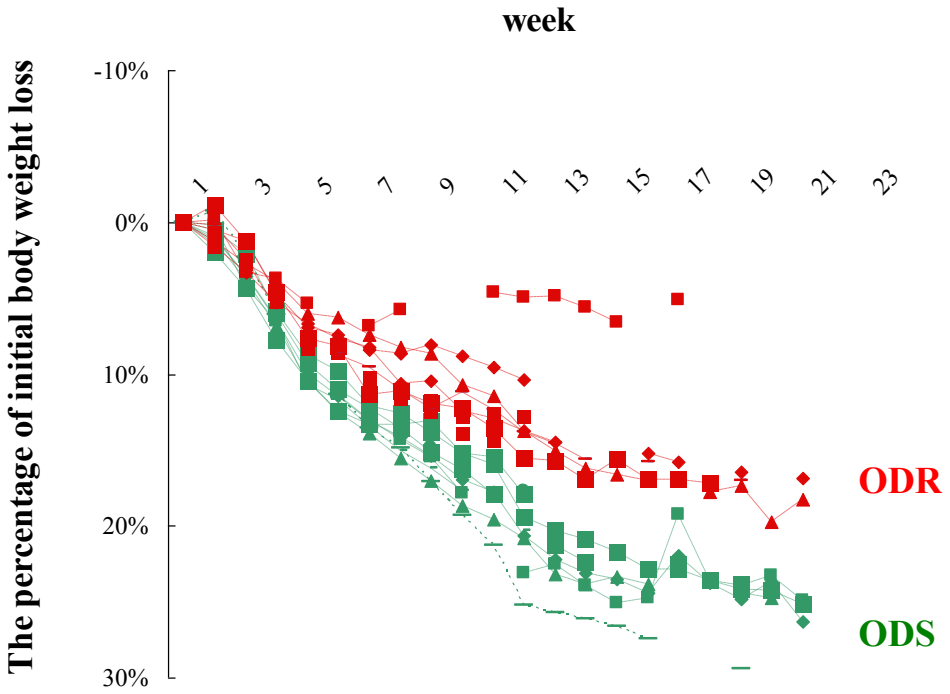
week
The percentage of initial body weight loss
-10%
0%
10%
20%
30%
1
3
5
7
9
11
13
15
17
19
21
23
ODR
ODS

IN VITRO MODEL

To confirm the purity of human primary myoblasts after isolation from muscle tissue, desmin, a specific protein expressed in muscle cells, was assessed by immunofluorescent staining. Immunofluorescent staining showed that more than 95% of the cells (labeled) were myogenic (desmin positive) after isolation (Figure 3.2-1). To verify that myoblasts were properly differentiated into myotubes in LG or HG differentiation medium, protein levels of myosin heavy chain (MHC) isoforms, markers of myotube differentiation, were measured by Western blot. Western blots confirmed that both slow and fast MHC protein levels increased during myoblast differentiation (Figure 3.2-2(A)) and that there was no difference in the proportion of sMHC and fMHC in the myotubes between ODS and ODR patients (Figure 3.2-2(C)).

In addition, the expression of sMHC of ODS myotubes was significantly higher in HG than in LG differentiation medium. There was a trend of higher sMHC expressed in HG than LG in ODR myotubes but it was not statistically significant (Figure 3.2(B), (D)). Therefore, there was a higher degree of differentiation of myoblasts in HG than in LG differentiation medium.

Figure 3.2-1: Purity of satellite cells after immunoselection. Immunofluorescence was measured with monoclonal mouse-anti human desmin primary antibodies and secondary antibodies conjugated to Texas Red, and followed by DAPI for nucleus staining. (Before immunoselection) ~50% of the cells are desmin (red) positive. More than 95% cells are desmin (red) positive after immunoselection of CD-56-positive satellite cells (labelled). Non myogenic cells (unlabelled) were only DAPI (blue) stained.

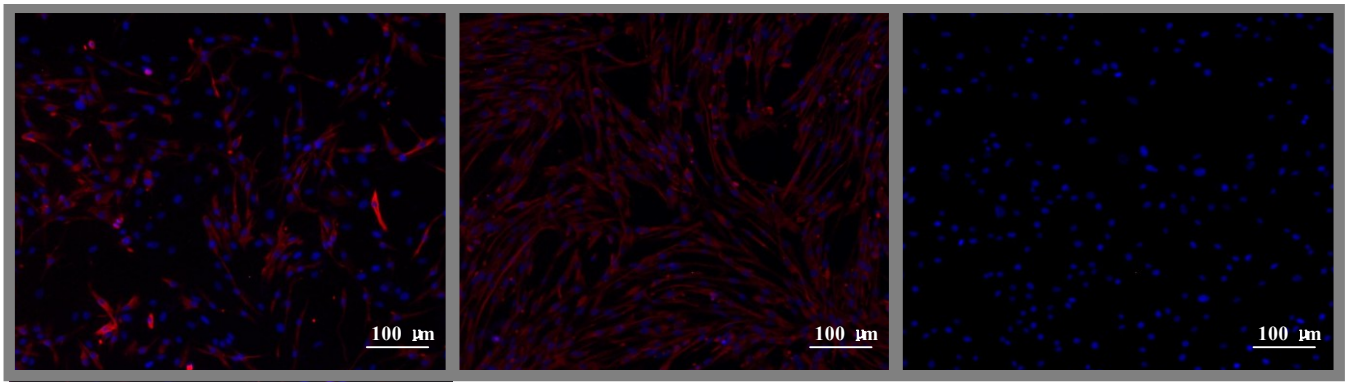

(Before immunoselection) **Labelled** **Unlabelled**

Figure 3.2-2: MHC expression of myotubes. (A) Cellular protein was extracted from the cultures of myoblasts and myotubes on days +0, +2, +4 and +6 of differentiation in LG differentiation media, electrophoresed, immunoblotted, and probed using mAbs S58 (sMHC) or F59 (fMHC) (B) Western blot analysis of sMHC and fMHC in representative human myotubes of ODS and ODR patients. Myoblasts were differentiated in LG or HG differentiation Medium. (C) Quantification by density analysis of sMHC and fMHC expression. Data are presented as the sMHC/fMHC ratio. (D) Quantification by density analysis of sMHC expression. Data are presented as the sMHC/beta-actin ratio. *P<0.05, LG *vs.* HG (ODS) Data are shown as mean ±SEM n=4. sMHC: slow myosin heavy chain; fMHC: fast myosin heavy chain

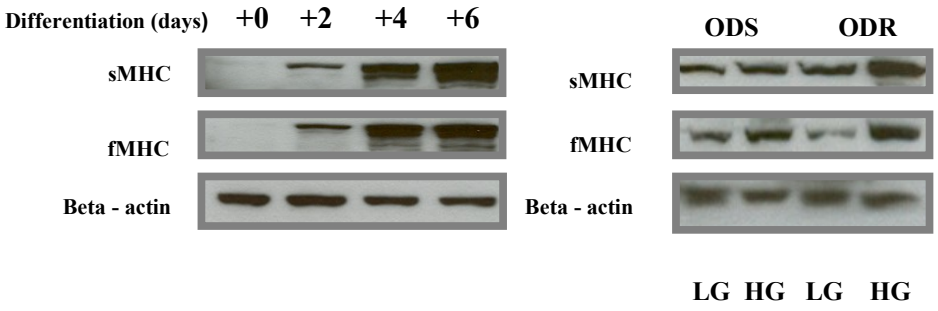
Differentiation (days)
+0
+2
+4
+6
sMHC
fMHC
Beta - actin
ODS
ODR
sMHC
fMHC
Beta - actin
LG HG LG HG

(A) (B)

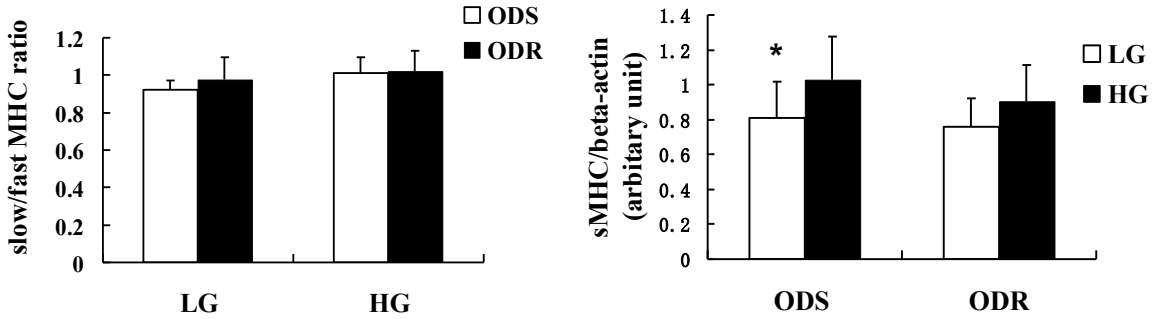
slow/fast MHC ratio
1.2
1
0.8
0.6
0.4
0.2
0
ODS
ODR
LG
HG
sMHC/beta-actin (arbitary unit)
1.4
1.2
1
0.8
0.6
0.4
0.2
0
*
LG
HG
ODS
ODR

(C) (D)

MITOCHONDRIAL METABOLIC ANALYSIS

To assess metabolic characteristics of the differentiated myotubes from ODS and ODR patients, mitochondrial oxygen consumption rate (OCR) was measured under resting, oligomycin-induced (State 4) and maximal (FCCP induced) conditions. Oxygen consumption in the absence of ADP phosphorylation (i.e., when ATP synthase is inhibited by oligomycin) was used to directly measure mitochondrial proton leak-dependent respiration. There was no significant difference in resting or maximal OCR between ODS and ODR myotubes (Figure 3.3-1(A), 3.3-1(D, E)). However, State 4 and State 4/Resting OCR was significantly lower ($P < 0.05$) in ODR compared to ODS myotubes (Figure 3.3-1(B, C)).

Extracellular acidification rate (ECAR) was measured under resting conditions and following the addition of oligomycin. ECAR, which measures extracellular changes in pH, is an indirect estimation of lactic acid production from cellular glycolysis. Inhibition of oxidative phosphorylation by oligomycin increases the conversion of pyruvate into lactate since cells become reliant on glycolytic ATP production. There were no significant differences in resting and oligomycin-induced (State 4) ECAR values between ODS and ODR myotubes (Figure 3.3-2(A, B)). However, after oligomycin treatment, the fold increase of ECAR (State 4/Resting) was significantly higher in ODR compared to ODS myotubes in HG medium ($P<0.05$) (Figure 3.3-2(C)). This result indicates that ODR myotubes had a higher capacity to switch to glycolysis in HG medium compared with ODS myotubes. In addition, there was no difference between ODS and ODR myotubes in terms of cellular ATP levels (Figure 3.3-3). Cellular ATP levels were measured using a conventional luciferase/luciferin ATP detection system.

Figure 3.3-1: Oxygen consumption rates of myotubes from ODS and ODR patients. (A) Resting oxygen consumption rate (OCR). (B) State 4 OCR (leak-dependent OCR). (C) State 4/resting OCR. (B-C) After the resting OCR measurement, oligomycin (500ng/mL) was injected into the wells to determine state 4 OCR. *P<0.05, ODS *vs.* ODR (LG and HG) (D) Maximal OCR. (E) Maximal/Resting OCR. (D-E) After resting and state 4 OCR, mitochondrial maximal phosphorylation capacity was measured following injection of FCCP (1uM) (A-E) Human primary myoblasts were differentiated into human myotubes for 6 days in LG (5 mM glucose) and HG (25 mM glucose). Results are presented as means ± SEM, n=6, where each condition was assessed in 5-8 replicates.

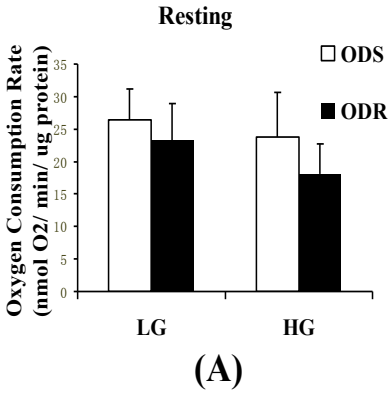
Resting
ODS
ODR
Oxygen Consumption Rate
(nmol O2/ min/ ug protein)
35
30
25
20
15
10
5
0
LG
HG

(A)

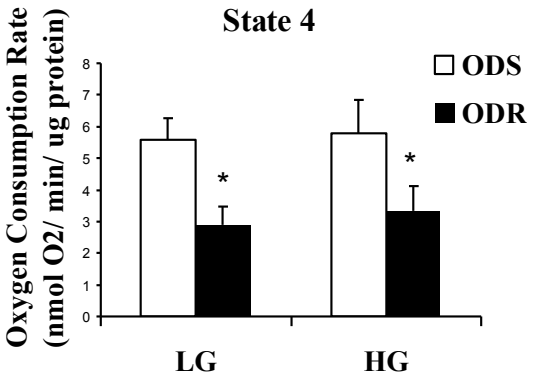
State 4
ODS
ODR
Oxygen Consumption Rate
(nmol O2/ min/ ug protein)
8
7
6
5
4
3
2
1
0
*
*
LG
HG

(B)

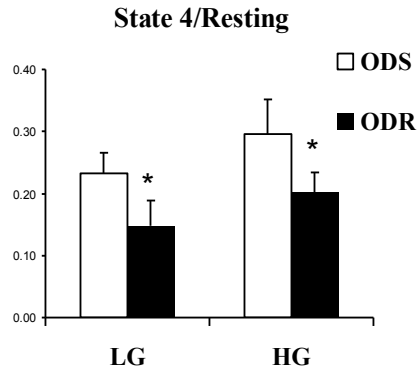
State 4/Resting
ODS
ODR
0.40
0.30
0.20
0.10
0.00
*
*
LG
HG

(C)

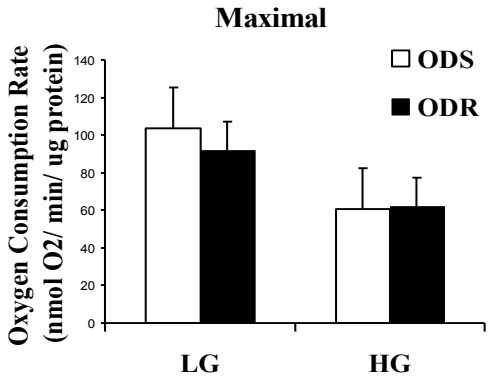
Maximal
ODS
ODR
Oxygen Consumption Rate
(nmol O2/ min/ ug protein)
140
120
100
80
60
40
20
0
LG
HG

(D)

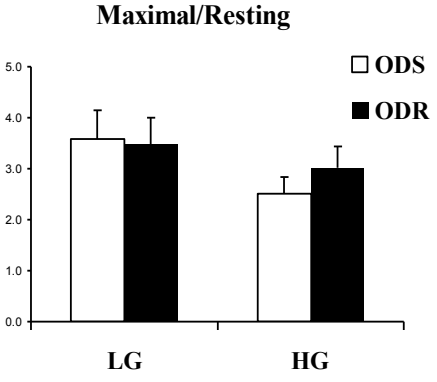
Maximal/Resting
ODS
ODR
5.0
4.0
3.0
2.0
1.0
0.0
LG
HG

(E)

Figure 3.3-2: Glycolytic capacity of myotubes from ODS and ODR patients. (A) Resting extracellular acidification rate (ECAR). (B) Oligomycin induced ECAR. (C) Fold increase of ECAR (State 4/Resting). Switch from oxidative to glycolytic metabolism after inhibition of ATP synthase by oligomycin. (A-C) Human primary myoblasts were differentiated into human myotubes for 6 days in LG (5 mM glucose) and HG (25 mM glucose). *P<0.05, ODS *vs.* ODR HG Results are presented as means ± SEM, n=6, where each condition was assessed in 5-8 replicates.

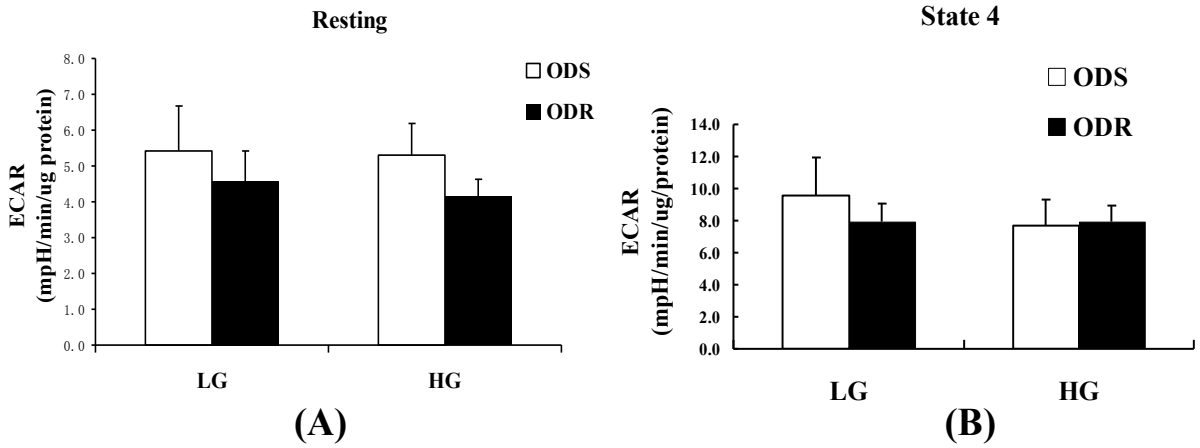
Resting
ECAR
(mpH/min/ug protein)
8.0
7.0
6.0
5.0
4.0
3.0
2.0
1.0
0.0
ODS
ODR
LG
HG
(A)
State 4
ECAR
(mpH/min/ug/protein)
14.0
12.0
10.0
8.0
6.0
4.0
2.0
0.0
ODS
ODR
LG
HG
(B)

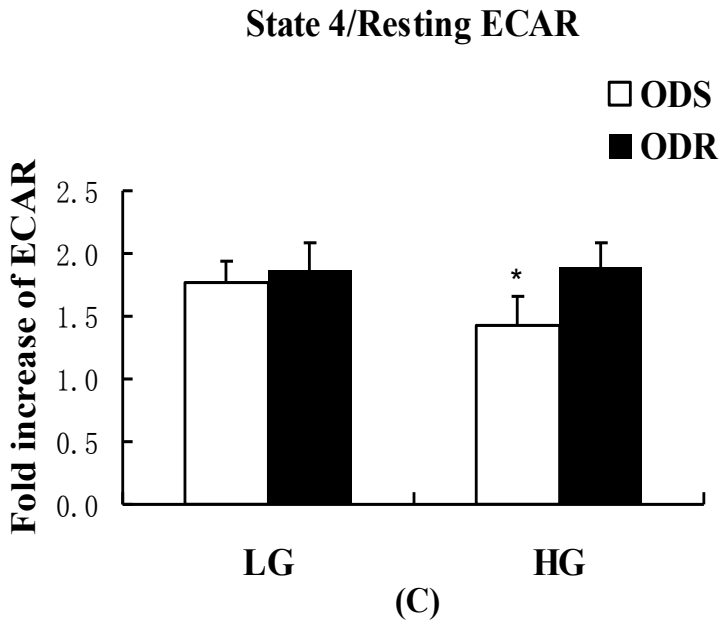
State 4/Resting ECAR
ODS
ODR
Fold increase of ECAR
2.5
2.0
1.5
1.0
0.5
0.0
*
LG
HG
(C)

Figure 3.3-3: ATP content of myotubes from ODS and ODR patients. ATP content in myotubes from ODS and ODR subjects differentiated for 6 days in LG (5mM glucose) and HG (25mM glucose). Results are presented as means ± SEM, n=6, where each condition was assessed in triplicate.

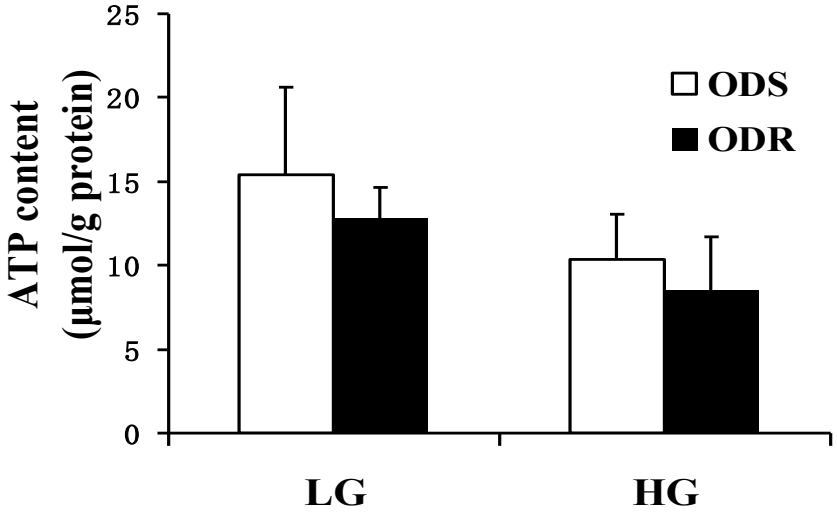
ATP content
(μmol/g protein)
25
20
15
10
5
0
ODS
ODR
LG
HG

Mitochondrial Content

To verify whether the proton leak and glycolytic capacity differences between ODS and ODR myotubes were due to a difference in mitochondrial content, the mitochondrial content was assessed by the mitochondrial-selective fluorescent probe, Mitotracker Green, and by the levels of two mitochondrial proteins (Complex III and SDH). There was no observable difference in the mitochondrial network in cultured myotubes from ODS and ODR patients (Figure 3.4-1). In addition, there was no significant difference in mitochondrial protein levels between ODS and ODR myotubes (Figure 3.4-2). However, mitochondrial content was variable from sample to sample (Western blot results), and there was a trend of higher mitochondrial protein level in ODS compared to ODR myotubes. It is necessary to increase the sample size to determine definitively whether there is a significant difference in mitochondrial content between ODS and ODR patients.

Mitochondrial Membrane Potential

To further elucidate the mechanism of metabolic difference between ODS and ODR myotubes, mitochondrial membrane potential was measured by TMRE. There was no difference in resting mitochondrial membrane potential (Figure 3.5-1) and oligomycin-induced mitochondrial membrane potential (data not shown) between ODS and ODR myotubes. There was higher mitochondrial membrane potential in LG than HG media for both ODS and ODR myotubes (Figure 3.5-1). FCCP depolarizes mitochondrial inner membranes and therefore, net TMRE fluorescence was increased dramatically after FCCP injection (Figure 3.5-1).

Figure 3.4-1: Mitochondrial morphology in myotubes from ODS and ODR patients. Representative Mitotracker Green staining in one of the six 6 pairs of ODS and ODR myotubes differentiated in LG or HG differentiation media for 6 days. Mitochondria were stained with 250 nM Mitotracker Green and visualized using a fluorescence microscope. Top panel: ODS myotubes differentiated in LG and HG media. Botton panel: ODR myotubes differentiated in LG and HG media.

ODS

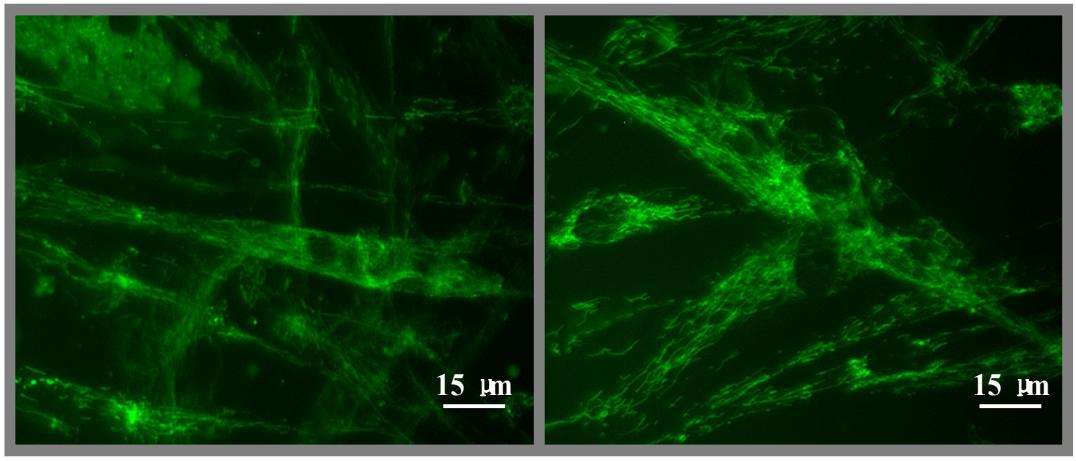

LG **HG**

ODR

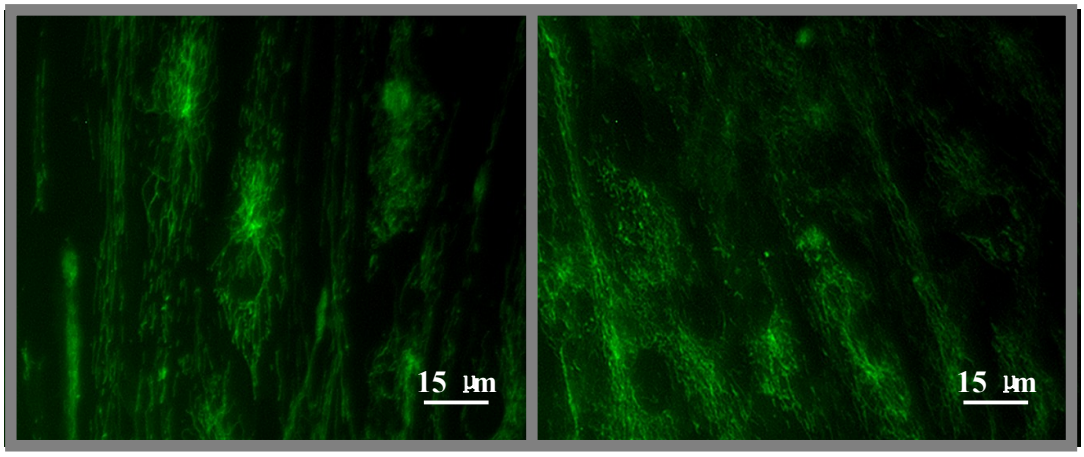

LG **HG**

Figure 3.4-2: Mitochondrial content of myotubes from ODS and ODR patients. Mitochondrial content was measured by Western blot for Complex III (core I subunit) of the ETC and succinate dehydrogenase (SDH) in myotubes differentiated in LG or HG media from ODS and ODR subjects. (A): Representative Western blot of Complex III (core I subunit) and SDH levels. Beta-actin was used as a loading control. (B): Quantification by density analysis of Complex III (core I subunit) and SDH levels. Data are presented normalized to beta-actin protein level. Data are shown as mean±SEM, Complex III n=6; SDH n=4.

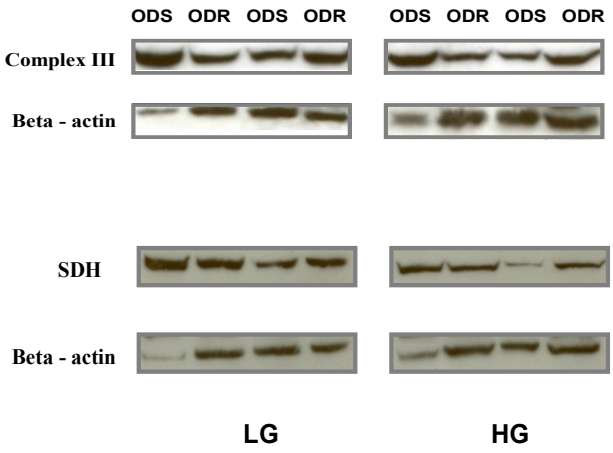
ODS ODR ODS ODR
ODS ODR ODS ODR
Complex III
Beta - actin
SDH
Beta - actin
LG
HG

(A)

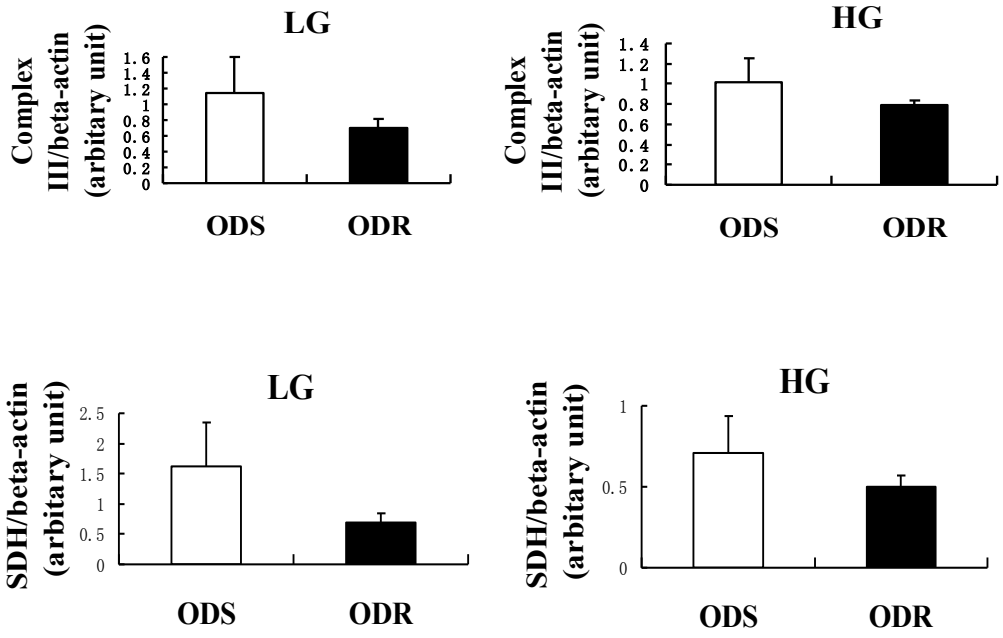
LG
Complex III/beta-actin (arbitary unit)
1.6
1.4
1.2
1
0.8
0.6
0.4
0.2
0
ODS
ODR
HG
Complex III/beta-actin (arbitary unit)
1.4
1.2
1
0.8
0.6
0.4
0.2
0
ODS
ODR
LG
SDH/beta-actin (arbitary unit)
2.5
2
1.5
1
0.5
0
ODS
ODR
HG
SDH/beta-actin (arbitary unit)
1
0.5
0
ODS
ODR

(B)

Figure 3.5-1: Mitochondrial membrane potential of myotubes from ODS and ODR patients. (A) Representative TMRE staining of myotubes differentiated in HG differentiation media for 6 days. Mitochondria were stained with 800nmol/L TMRE and visualized using a fluorescence microscope. Resting mitochondrial membrane potential: (no inhibitors or uncouplers); Olygomycin induces inner-membrane polarization and FCCP induces inner-membrane depolarization. (B) Myotubes were incubated with TMRE (175 nmol/L) in LG or HG PBS. Net increase of TMRE fluorescence (excitation 544 nm, emission 590nm) was measured in cultured myotubes from ODS and ODR patients. Human primary myoblasts were differentiated into human myotubes for 6 days in LG (5 mM glucose) and HG (25 mM glucose) media. # $P<0.05$ FCCP effect; *$P<0.05$ LG *vs*. HG differentiation media effect. Data are shown as mean ±SEM, n=6

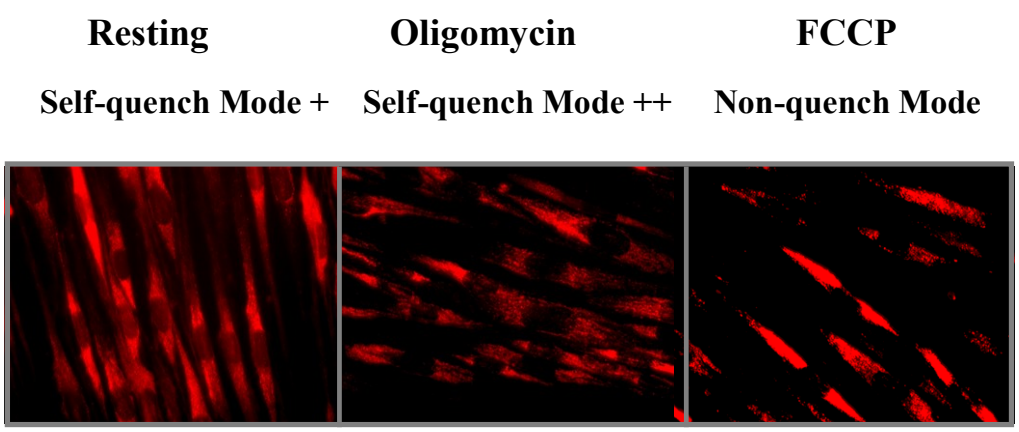
Resting
Oligomycin
FCCP
Self-quench Mode +
Self-quench Mode ++
Non-quench Mode

(A)

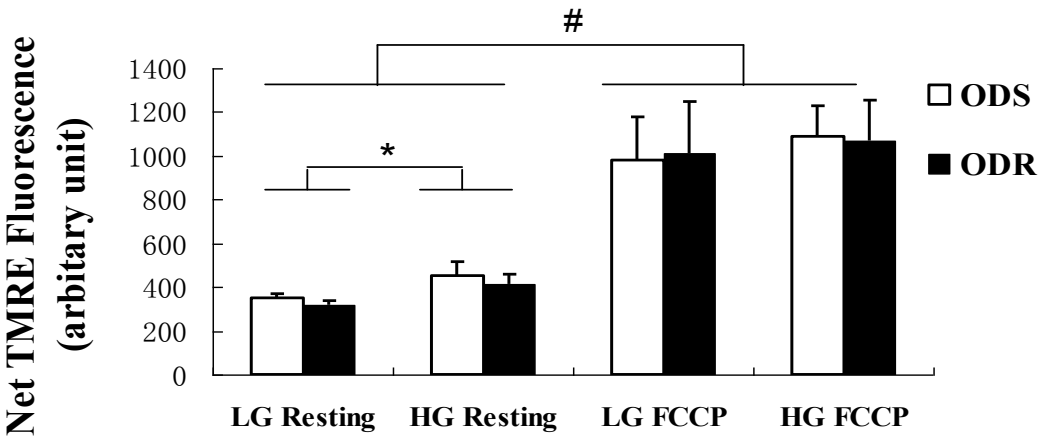
Net TMRE Fluorescence (arbitary unit)
1400
1200
1000
800
600
400
200
0
#
*
ODS
ODR
LG Resting
HG Resting
LG FCCP
HG FCCP

(B)

CELLULAR OXIDATIVE STRESS

Since mitochondrial membrane potential is usually correlated with mitochondrial ROS emission, cellular ROS levels were measured between ODS and ODR myotubes. There was no significant difference of cellular ROS levels between these two groups (Figure 3.5-2). Since cellular ROS is highly regulated by several anti-ROS systems, SOD2 (MnSOD) protein levels were measured in ODS and ODR myotubes by Western blotting. Western blots of MnSOD showed that ODS myotubes had significantly lower MnSOD levels than ODR myotubes in LG medium ($p<0.05$) (Figure 3.5-3).

To further identify whether differences in mitochondrial proton leak between ODS and ODR myotubes were related with protein expression of UCP3, UCP3 protein levels were measured by Western blotting. However, there was no significant difference of UCP3 protein levels between ODS and ODR myotubes in LG or HG medium (Figure 3.5-4).

Figure 3.5-2: ROS levels of myotubes from ODS and ODR patients. Myotubes from ODS and ODR patients were differentiated in LG or HG media for 6 days. ROS levels were determined with DCFH-DA (20uM, 30min exposure). Data were normalized to cellular protein level. Data are shown as mean±SEM n=6

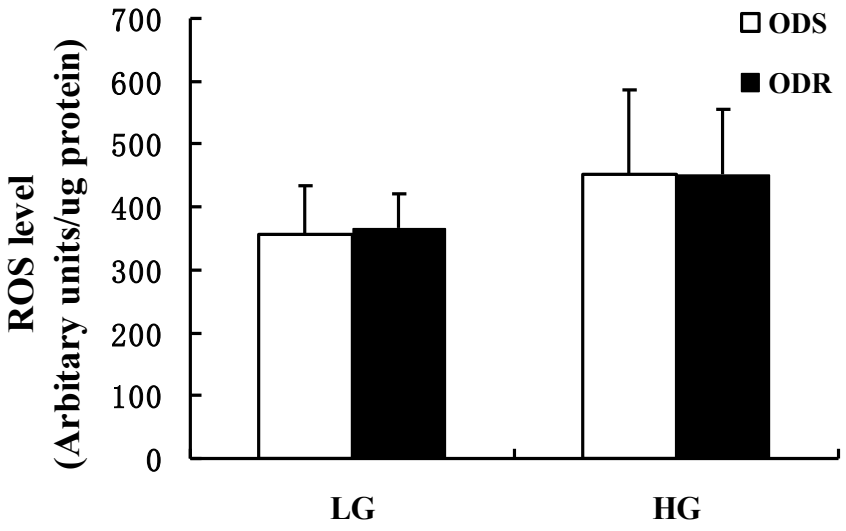
ROS level
(Arbitary units/ug protein)
700
600
500
400
300
200
100
0
ODS
ODR
LG
HG

Figure 3.5-3: MnSOD levels of myotubes from ODS and ODR patients. MnSOD levels were measured by Western blot analyses of myotubes from ODS and ODR subjects. (A): Representative Western blot of MnSOD levels in LG differentiation medium. Complex III was used as a mitochondrial content control. (B): Quantification by density analysis of MnSOD levels in LG medium. *P<0.05, ODS *vs.* ODR in LG Data are presented normalized to Complex III protein level. Data are shown as mean±SEM, n=4.

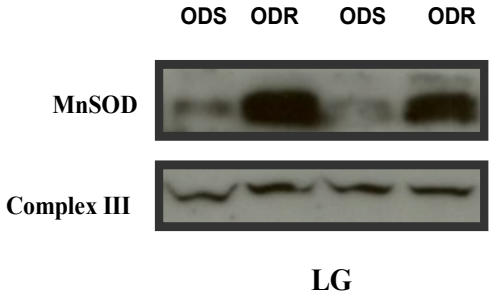
ODS
ODR
ODS
ODR
MnSOD
Complex III
LG

(A)

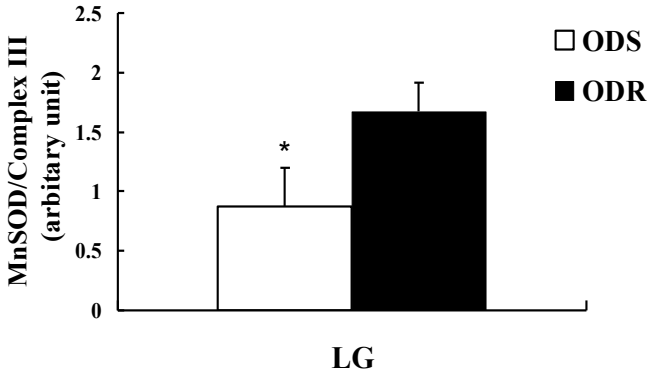
MnSOD/Complex III
(arbitary unit)
2.5
2
1.5
1
0.5
0
*
ODS
ODR
LG

(B)

Figure 3.5-4: UCP3 levels of myotubes from ODS and ODR patients. UCP3 levels were measured by Western blot analyses of myotubes from ODS and ODR subjects. (A): Representative Western blot of UCP3 levels in LG or HG media. α-tubulin was used as a loading control. (B): Quantification by density analysis of UCP3 levels in LG and HG differentiation media. Data are presented normalized to α-tubulin expression. Data are shown as mean±SEM, n=6.

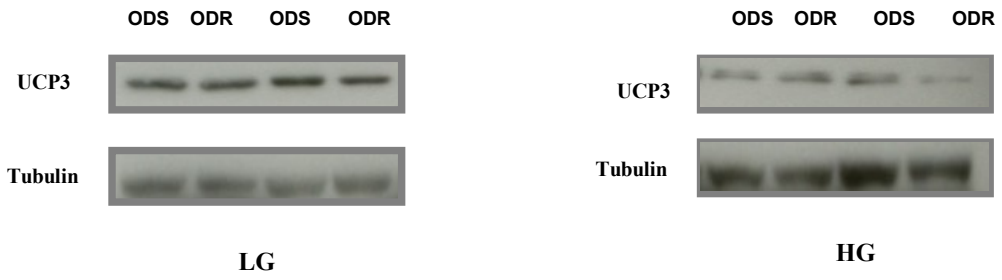
ODS ODR ODS ODR
UCP3
Tubulin
LG
ODS ODR ODS ODR
UCP3
Tubulin
HG

(A)

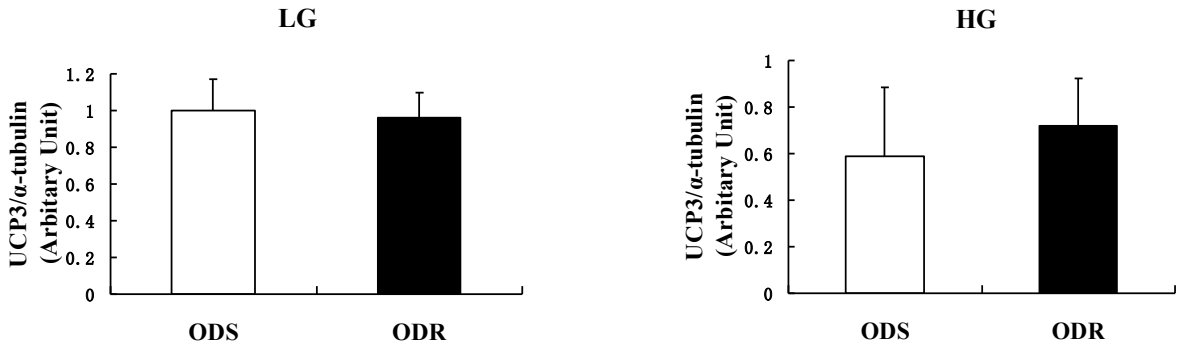
LG
UCP3/α-tubulin (Arbitary Unit)
1.2
1
0.8
0.6
0.4
0.2
0
ODS
ODR
HG
UCP3/α-tubulin (Arbitary Unit)
1
0.8
0.6
0.4
0.2
0
ODS
ODR

(B)

CHAPTER FOUR - GENERAL DISCUSSION

SUMMARY

The overall goal of this research was to study the metabolic characteristics of primary myotubes from obese patients having vastly different rates of weight loss in the Ottawa Hospital Weight Management Clinic. As previous studies have shown that proton leak-dependent oxygen consumption in skeletal muscle (*rectus femoris*) was 50% higher in mitochondria from ODS compared with that in ODR mitochondria, we hypothesize that mitochondrial proton leak is an important determinant of weight loss success. For my research, primary myoblasts were isolated from *vastus lateralis* muscle biopsies of ODS and ODR patients for this *in vitro* study of myotube metabolic characteristics. Mitochondrial leak-dependant OCR was found to be significantly higher ($P < 0.05$) in ODS compared to ODR myotubes, whether cells were differentiated in low or high glucose media. In addition, ODR myotubes had higher levels of MnSOD in LG medium. MnSOD is a mitochondrial matrix protein that is important in the prevention of cellular oxidative stress. There were no significant differences in mitochondrial content, mitochondrial membrane potential, cellular ROS levels or ATP content between ODS and ODR myotubes. Therefore, our *in vitro* results from myotubes are consistent with our previous *ex vivo* results of increased proton leak in mitochondria from muscle of ODS patients compared to ODR patients.

PRIMARY MYOTUBES: AN *IN VITRO* MODEL FOR STUDYING HUMAN MUSCLE METABOLISM

Muscle satellite cells were first described in 1961 using electron microscopy; they were identified as mononucleated cells juxtaposed between the sarcolemma of a muscle fiber and the basement membrane surrounding the fiber (Mauro *et al.* 1961). Such a microenvironment anatomical compartment, or 'niche', maintains satellite cells in a quiescent state with limited gene expression and protein synthesis (Le Grand *et al.* 2007). These satellite cells can become activated to divide and/or differentiate in response to stresses such as extrinsic injury or muscle growth and repair (Le Grand *et al.* 2007). Quiescent satellite cells in freshly isolated muscle tissue preparations can be activated immediately during muscle processing and are referred to as myogenic precursor cells, or myoblasts (Rando and Blau 1994). They then migrate away from the niche, cross the basement membrane, and either proliferate into myoblasts or differentiate into myotubes, respectively (Kuang *et al.* 2006, Shefer *et al.* 2004).

Many studies have used myotubes as an experimental system to probe metabolic characteristics of human muscle and the mechanistic origins of muscle pathologies. For example, Henry and colleagues showed that defective insulin-stimulated glucose transport persists in myotubes from T2DM subjects and resembles the reduced insulin-mediated glucose uptake present *in vivo* (Henry *et al.* 1995). In addition, myotubes from T2DM subjects had reduced palmitic acid oxidation and defects in glucose transport and glycogen synthase activity compared with control myotubes (Gaster *et al.* 2002, 2004). Moreover, Ukropcova and

colleagues demonstrated that subjects with a family history of T2DM were metabolically inflexible and had reduced high fat diet-induced fat oxidation and muscle mitochondrial content, indicating that such metabolic switching from carbohydrate to fat oxidation is an intrinsic characteristic of skeletal muscles (Ukropcova *et al.* 2005, 2007). A paper published previously from our lab showed that myotubes from patients with a history of T2DM were unable to increase oxidative capacity and had increased cellular oxidative damage when incubated in HG (25mM glucose) medium compared to myotubes from control subjects having no history of T2DM (Costford *et al*. 2009). Because such characteristics remain in myotubes, it is thought that they have genetic or epigenetic origins. Therefore, this *in vitro* model provides an experimental system enabling studies of potential intrinsic mechanisms to the skeletal muscle that may explain in part the ODS and ODR "phenotypes".

This research focused on the metabolic characteristics of differentiated myotubes of ODS and ODR patients. Human primary myoblasts were isolated from *vastus lateralis* biopsies of paired ODS and ODR patients and were induced to differentiate in LG and in HG differentiation media. In this study, State 4 OCR was significantly lower ($P < 0.05$) in ODR compared to ODS myotubes. This result was consistent with our previous published *ex vivo* data (Harper *et al.* 2002). Such an *in vitro* model provides a more physiological condition to assess the function of mitochondria within cells and also eliminates the influence of *in vivo* factors such as neuronal input, hormone concentrations, and physical activity. The main limitation of this *in vitro* model is that even though primary myoblasts are capable of differentiating into multinucleated myotubes, they have limitations as a model of *in vivo* muscle fibers. For example, human myotubes *in vitro* express embryonic, fetal, slow and fast MHC isoforms and are characterized as a

heterogeneous population of fiber types while human muscle only expresses slow and fast MHC isoforms (Mouly *et al.* 1993). In addition, muscle contraction occurs during physical exercise while cultured myotubes *in vitro* are normally in the resting state. Any characteristics related to muscle contraction are not likely to be observed in myotubes *in vitro*.

THE ROLE OF GLUCOSE ON THE METABOLISM AND DIFFERENTIATION OF PRIMARY MYOBLASTS

Skeletal muscle is a major site of whole body glucose metabolism, and is responsible for approximately 80% of insulin-sensitive glucose metabolism (Defronzo *et al*. 1981). Glucose is the major carbon source in both cellular anaerobic and aerobic metabolism. Evidence has shown that the cellular metabolic state plays a crucial role in protein activation and protein post-translational modification (Gatlik-Landwojtowicz *et al.* 2004, Vishwasrao *et al.* 2005). Therefore, it is rational to assume that the metabolic state may have a significant effect on primary myoblasts differentiation since protein activation and post-translational modification are crucial during cell differentiation.

A paper published by Nedache *et al.* confirmed the importance of glucose levels in the regulation of myogenesis of C2C12 myotubes (Nedache *et al.* 2008). First, they observed that the process of C2C12 myogenesis was significantly delayed under LG (5 mM glucose) conditions compared with HG (22.5mM glucose) conditions on day four of differentiation. In addition, they

also noticed that SIRT1 (silent mating type information regulation 2 homolog 1) accumulated in the nucleus under the LG condition compared to the HG condition. This indicates that SIRT1 abundance and localization is sensitively influenced by glucose levels. SIRT1 is an energy and oxidation sensor; it is involved in the nutritional regulation of gene transcription in different tissues, including skeletal muscle. Moreover, Fulco and colleagues showed that overexpression of SIRT1 inhibited myogenesis, further confirming that SIRT1 plays an important role in myogenesis (Fulco *et al.* 2003). Interestingly, they also noticed that extracellular glucose concentrations decreased to less than 0.5 mM after a 24h incubation of C2C12 cells in LG (5mM), indicating that myotubes consume great amounts of glucose as an energy source (Nedache *et al.* 2008). Therefore, it is possible that myotubes studied under LG conditions for 24h create an environment that is similar to glucose starvation. Another relevant paper by Cantó and colleagues studied the role of the AMP-activated protein kinase (AMPK) in C2C12 myotubes in response to fasting-like conditions (Cantó *et al.* 2010). Consistently, LG (5mM) medium was used in their study as a glucose restricted condition in which AMPK and acetyl-CoA carboxylase (ACC) were activated by phosphorylation. However, these changes were rapidly reversed by re-incubating myotubes in HG (25mM) medium. Moreover, PGC-1α and FOXO1, two SIRT1-target and transcriptional regulators, were also downregulated by the inactivity of AMPK. Taken together, these papers provide good evidence to show that skeletal muscle cells were able to sense the limitation in glucose availability. Muscle cells respond to such fasting-like conditions through modulating the cellular redox sensors such as SIRT1 and AMPK. Activation/inactivation of these cellular redox sensors plays a crucial role in the regulation of the gene expression of muscle cell myogenesis.

In this study, primary myoblasts were differentiated in both LG (5mM) and HG (25mM) differentiation media for 6 days. Myotubes from ODS patients were differentiated significantly more ($P<0.05$) in HG medium compared to LG medium. There was the same trend for myotubes from ODR patients, but this was not statistically significant. One explanation is that ODS myotubes may be more sensitive metabolically to glucose levels than ODR myotubes. It should be noted, however, that primary muscle cells and C2C12 cells may not have the same level of insulin responsiveness. Previous studies showed that C2C12 cells have low levels of GLUT4 proteins, and have poor insulin responsiveness even after differentiation (Kotliar *et al.* 1992, Sargeant *et al.* 1993). The LG (5mM glucose) conditions in this study mimicked *in vivo* physiological blood glucose levels before meals while the HG (25mM glucose) conditions were used to mimic *in vivo* chronic hyperglycemia. However, as described above, LG (5mM glucose) conditions for C2C12 cells elicit cell starvation-like responses. Therefore, achieving an appropriate glucose concentration in experimental media is important for the use of primary cultures of human muscle myoblasts.

MITOCHONDRIAL PROTON LEAK

In this study, the major finding was that mitochondrial proton leak was significantly lower in ODR compared to ODS myotubes. This is consistent with our previously published *ex vivo* data, in which analyses were conducted in mitochondria from *rectus femoris* of paired ODS and ODR patients (Harper *et al.* 2002). While the mechanisms of proton leak are still poorly understood, as early as 1997, Nègre-Salvayre *et al.* showed that inhibition of UCP2 in rat hepatocytes by

GDP increased mitochondrial ROS production (Nègre-Salvayre *et al.* 1997). Later on, Brand and colleagues proposed that "mild uncoupling" caused by mitochondrial proton leak is one of the mechanisms for the mitigation of mitochondrial ROS production (Echtay *et al.* 2002, Brand *et al.* 2005). As mentioned in chapter one, ANT and the UCPs contribute to mitochondrial proton leak. ANT-mediated mitochondrial proton leak has recently been implicated as a consequence of abnormally high levels of ROS and/or an overload of Ca^{2+} leading to mitochondrial inner membrane depolarization and apoptosis (Nadtochiy *et al.* 2006). It is widely accepted that ANT is a core protein of the permeability transition pore (PTP), a non-specific large pore in the mitochondrial inner membrane (Schwarz *et al.* 2007). Moreover, ANT is activated by 4-HNE, a highly toxic membrane lipid by-product of oxidative stress (Aguirre *et al.* 2010). In addition, Nadtochiy and colleagues have shown that mitochondrial proton leak through ANT was controlled by covalent modification of cysteine residues in ANT, and such an activation of ANT-mediated proton leak resulted in cell death (Nadtochiy *et al.* 2006). Therefore, it is likely that ANT-mediated proton leak is not involved in the mechanism of mitigating ROS production.

Mitochondrial ROS production can be mitigated by increased mitochondrial proton leak associated with UCP2 and UCP3. El-Khoury and colleagues showed that increased ROS production in macrophages upregulated UCP2 expression, consistent with the idea that UCP2 is a constitutive modulator of ROS production in macrophage-mediated immunity (El-Khoury *et al.* 2011). In addition, Toime and colleagues further confirmed that UCP3 actively lowers ROS production in isolated skeletal muscle mitochondria and showed that the UCP3-specific activity lowered ROS level 90-500 times more than that the activity associated with ANT (Toime *et al.*

2010). However, evidence does not support the idea that UCP1 is involved in the regulation of ROS production (Shabalina *et al.* 2010). It is possible that the redox environment differences between BAT and skeletal muscle affect the regulation of ROS production by the UCPs (Mailloux *et al.* 2011b).

Although higher mitochondrial proton leak was observed in ODS myotubes, there was no difference in UCP3 protein expression levels between ODS and ODR myotubes. It is thus possible that the differences in mitochondrial proton leak between ODS and ODR myotubes is due to an increase in UCP3 protein activity. As discussed, there is good evidence that UCPs can be activated directly by superoxide by-products to induce mitochondrial proton leak, and attenuating ROS production. A recent paper published from our lab showed that protein glutathionylation/deglutathionylation plays a very important role in regulating ROS-induced mitochondrial proton leak through UCP2 and UCP3, but not UCP1 (Mailloux *et al.* 2011a). In addition, Mailloux *et al.* were able to identify Cys^{25} and Cys^{259}, which are found in the first membrane spanning domain and a loop region that contacts the matrix, respectively, as possible chief sites for UCP3 glutathionylation. UCP3-induced proton leak was also inhibited by diamide, a catalyst of glutathionylation. Also, GRx1 was shown to covalently conjugate GSH to purified UCP3 *in vitro*, implying that the reaction of glutathionylation of UCPs could be catalyzed enzymatically *in vivo*.

In addition, a recently published paper showed that Trx2 interacted with UCP3 and inhibited UCP3, consistent with our findings that the activation of UCP3 is regulated by cellular redox states (Hirasaka *et al.* 2011). Moreover, only slightly increased ROS levels are required to

elevate State 4 respiration in UCP3 wild-type myotubes and there was no response in UCP3 knockout cells, indicating that only small amounts of ROS are needed to activate proton leak through UCP3 (Mailloux *et al.* 2011a). In addition, the ROS-mediated activation of UCP3 was reversed by glutathionylation. Mailloux *et al.* showed that the deglutathionylation of UCP3 is required to diminish ROS emissions from skeletal muscle mitochondria through a proton leak mechanism (Mailloux *et al.* 2011a). Similar observations were made relating to UCP2 (Mailloux *et al.* 2011a). According to these mechanistic data, we hypothesize that the significant differences in mitochondrial proton leak between ODS and ODR myotubes is related to variations in UCP3 activation by cellular redox states. Results suggest that under normal ROS levels, UCP3 is partially glutathionylated and that small increases in ROS induce the activation of UCP2 and UCP3 by deglutathionylation. Therefore, the activation of UCP3 between ODS and ODR needs to be further studied. For example, cellular redox state (GSH/GSSG) and the ratio of glutathionylation/degultathionylation of UCP3 status are specific issues requiring analysis.

ROS & ANTI-OXIDANT SYSTEMS

In this study, there was no significant difference in ROS levels between ODS and ODR myotubes. The DCFH-DA assay was used in this study to detect cellular ROS levels. The principle of this method is that DCFH emits fluorescence only after being oxidized predominantly by H_2O_2. The strength of this assay is that DCFH-DA is membrane permeable, and therefore allows the measurement of ROS in intact cells. However, since the DCFH-DA assay detects only H_2O_2, and not superoxide ($O_2^{\bullet -}$), it is not very sensitive to rapid changes of superoxide ($O_2^{\bullet -}$) in the cell

(Rhee *et al.* 2010). In addition, DCFH does not react with other free radicals such as nitric oxide ($NO^{\bullet}$), peroxyl radicals ($ROO^{\bullet}$) and the hydroxyl radical ($^{\bullet}OH$). Superoxide ($O_2^{\bullet-}$) and its dismutated product, H_2O_2, are kept at low concentrations because of the activity of the various anti-oxidant processes in mitochondria, but these concentrations can increase when mitochondrial membrane potential is elevated (Murphy *et al.* 2009, Seifert *et al.* 2010, Mailloux *et al.* 2011a). Our findings suggest that UCP2 and UCP3 are the 'first-responders' to slight increases in ROS production (Mailloux *et al.* 2011a).

Other methods recently used by others to obtain real-time measurements include a novel mitochondrial-targeted circularly permuted yellow fluorescent protein (mt-cpYFP), which displays significant increases in fluorescence by small changes in superoxide ($O_2^{\bullet-}$) (Wang *et al.* 2008). It is highly selective to superoxide ($O_2^{\bullet-}$), but is not affected by hydrogen peroxide (H_2O_2). By targeting cpYFP into the mitochondrial matrix, the detection of mitochondrial superoxide production is localized and captured by cpYEP flurorescence, termed as "superoxide flash" (Wang *et al.* 2008). It has been illustrated in a recent study and in other studies that superoxide flashes occur in a wide range of cell types, including isolated cardiac skeletal muscle cells, cultured neurons and intact heart (Wang *et al.* 2008, Pouvreau *et al.* 2010). In addition, Fang *et al.* recently generated a cpYEP transgenic mice and developed *in vivo* imaging techniques that allowed a kinetic observation of ROS production in muscles and sciatic nerves of living mice (Fang *et al.* 2011).

In this study, there was a significant increase in protein levels of MnSOD in ODR myotubes compared to ODS myotubes. It is worthy to note that oxidative stress is often associated with

increases in the conversion of glucose to lactate, since the ROS-mediated diminution of aerobic respiration necessitates increased ATP production from glycolysis (Mailloux *et al.* 2011c). In this study, we also observed that the fold increase of ECAR level was higher in ODR compared to ODS myotubes in HG, indicating that ODR myotubes had a higher capacity of glycolysis than ODS myotubes. Nishikawa *et al.* have also demonstrated that endothelial cells in HG (30mM) had accelerated rates of glycolysis, resulting in oversupply of pyruvate to the TCA cycle, causing excessive generation of ROS (Nishikawa *et al.* 2000). In this study, HG was used as a chronic condition since myoblasts were differentiated in HG for 6 days unlike the conditions used in Nishikawa *et al.* in which cells were incubated in HG for 2h. Since there was no significant increase of ROS under chronic HG condition in ODR myotubes, we therefore hypothesize that the higher MnSOD protein level in ODR myotubes may be the consequence of elevated ROS levels due to lower proton leak.

Consistent with the idea that the novel uncoupling proteins play a role in obesity, Walder and colleagues identified a significant association of UCP2 variants with metabolic rate during sleep and total energy expenditure in the Pima Indians in the South Western United States (Walder *et al.* 1998). In another study, the same group identified a novel polymorphism in the proximal promoter region of UCP3 which was associated with increased expression of UCP3 in skeletal muscle of non-diabetic male Pima Indians, indicating that low UCP3 mRNA expression may contribute to a low sleeping metabolic rate, a predisposing factor for weight loss failure (Schrauwen *et al.* 1999). Argyropoulos *et al*. showed that a missense mutation in exon 4 (C427T) and two polymorphisms in exon 3 (Val102Ile) and 6 (Ggt-Gat at the exon 6–splice donor

junction) in the UCP3 gene were identified in two severely obese probands (Argyropoulos *et al*. 1998). In addition, basal fat oxidation rates were reduced by 50% and respiratory quotient was significantly increased in exon 6 splice donor heterozygotes compared with control lean individuals, indicating a role for UCP3 in metabolic fuel partitioning. However, in previous studies of ODS and ODR patients, UCP3 mutations and polymorphisms were screened in both groups. There were no particular genotype identified that may be associated with differences in rate of weight loss (Harper *et al.* 2002). It is noteworthy that these previous results were from a limited number of patients and therefore may not reflect the small influence of genotype on the ability to lose weight among obese women.

How do these laboratory data accommodate the ODS and ODR whole body "phenotypes"? Subjects were classified as ODS and ODR on the basis of weight loss success in the first 6 weeks of the clinical weight loss program, when the low calorie diet was rigorously adhered to. As figure 4.1 shows, myotubes from ODS subjects have significantly higher mitochondrial proton leak, consistent with the idea that ODS subjects may mainly rely on proton leak rather than MnSOD to regulate cellular ROS levels. Therefore, ODR subjects who fail to lose as much weight as ODS subjects might have a dysregulated proton leak. Although the mechanism of mitochondrial proton leak is yet unknown, there is good evidence that about 50% of resting muscle energy expenditure is attributable to proton leak (Rolfe *et al.* 1996). Overall, it is estimated that mitochondrial proton leak accounts for about 20% of rat standard metabolic rate (Rolfe *et al.* 1999). Thus, if muscle energy expenditure accounts for about 20% of standard metabolic rate, observation of significant higher proton leak in ODS could possibly reflect a 5% difference in standard metabolic rate between ODS and ODR subjects.

Figure 4.1 Hypothetic model of the mechanism of increased UCP3-mediated proton leak in ODS compared to ODR muscle mitochondria MnSOD is the chief enzyme in the mitochondrial matrix converting $O_2^{\bullet-}$ to H_2O_2. Then H_2O_2 can be reduced to H_2O by glutathione peroxidase (GPx), and/or peroxiredoxin (PRx). UCP3 is activated by low levels of ROS, thus increasing proton leak-dependant respiration. Specifically, ROS cause the deglutathionylation of UCP3 to increase mitochondrial proton leak. In turn, this decreases protonmotive force, resulting in lower ROS levels. Findings reported in this thesis demonstrate that myotubes from ODS subjects have significantly higher mitochondrial proton leak, consistent with the idea that ODS subjects rely on proton leak to a greater extent than MnSOD to regulate cellular ROS levels than myotubes from ODR subjects. ODR subjects may have a dysregulated proton leak in skeletal muscle.

ODS

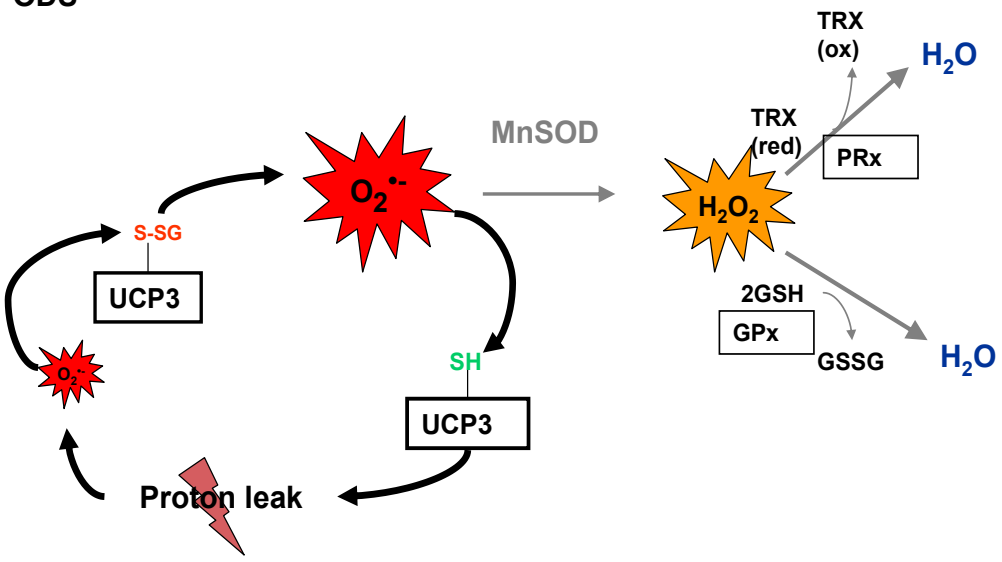
MnSOD
$O_2^{\bullet-}$
S-SG
UCP3
SH
UCP3
Proton leak
TRX (ox)
H_2O
TRX (red)
PRx
H_2O_2
2GSH
GPx
GSSG
H_2O

ODR

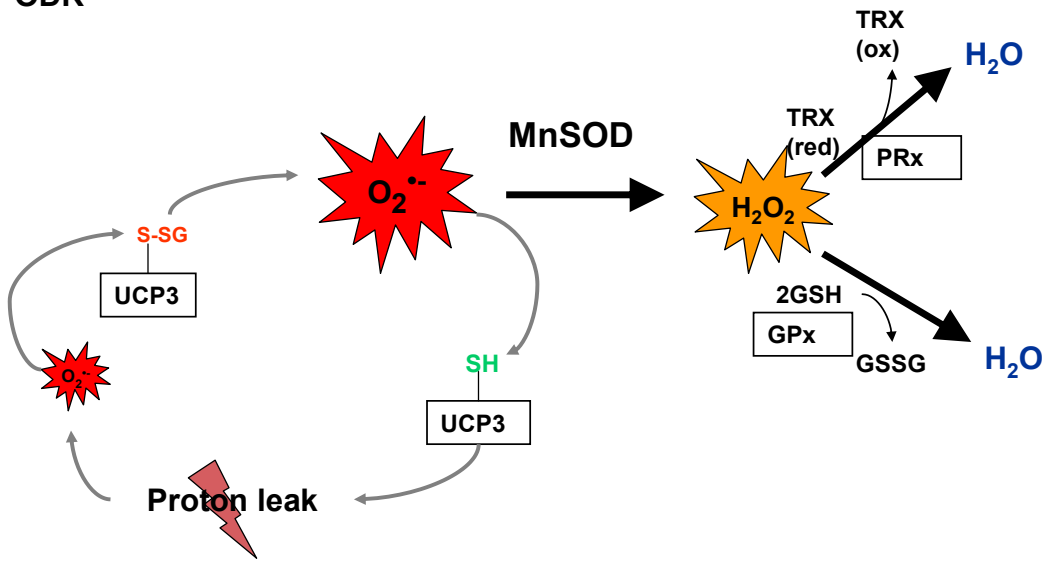
MnSOD
$O_2^{\bullet-}$
S-SG
UCP3
SH
UCP3
Proton leak
TRX (ox)
H_2O
TRX (red)
PRx
H_2O_2
2GSH
GPx
GSSG
H_2O

CONCLUSIONS

In summary, this dissertation demonstrates that there are significant intrinsic metabolic differences in the metabolism of primary muscle cells between ODS and ODR patients. The most significant finding in this study is that mitochondrial proton leak is significantly higher in ODS myotubes compared to ODR myotubes. The results from our *in vitro* model is consistent with our previous *ex vivo* results, further confirming that differences in skeletal muscle metabolism between ODS and ODR patients is genetically determined or has epigenetic origins. In addition, we showed that ODR myotubes have significantly higher MnSOD protein levels compared to levels in ODS myotubes. Therefore, it is rational to hypothesize that ODR subjects fail to lose as much weight as ODS subjects due in part to dysregulated proton leak. This work enhances our understanding of mitochondrial proton leak in the regulation of cellular ROS levels in myotubes from ODS and ODR groups. Although there have been tremendous improvements in our understanding of the genetic causes of obesity, there are still many unknowns. Certain patients have great difficulty in losing weight even though they are highly compliant to hypocaloric diets. These findings provide further insights into the metabolic mechanisms in skeletal muscle that contribute to the phenomenon of weight loss variability. Our findings may eventually lead to the development of interventions aimed at the prevention and/or treatment of obesity.

REFERENCES

Adrian TE, Ferri GL, Bacarese-Hamilton AJ, Fuessl HS, Polak JM, Bloom SR. Human distribution and release of a putative new gut hormone, peptide YY. Gastroenterology. 1985 89(5):1070-7.

Aguirre E, Cadenas S. GDP and carboxyatractylate inhibit 4-hydroxynonenal-activated proton conductance to differing degrees in mitochondria from skeletal muscle and heart. Biochim Biophys Acta. 2010 1797(10):1716-26.

Anderson EJ, Lustig ME, Boyle KE, Woodlief TL, Kane DA, Lin CT, Price JW 3rd, Kang L, Rabinovitch PS, Szeto HH, Houmard JA, Cortright RN, Wasserman DH, Neufer PD. Mitochondrial H2O2 emission and cellular redox state link excess fat intake to insulin resistance in both rodents and humans. J Clin Invest. 2009 119(3):573-81.

Argyropoulos G, Brown AM, Willi SM, Zhu J, He Y, Reitman M, Gevao SM, Spruill I, Garvey WT. Effects of mutations in the human uncoupling protein 3 gene on the respiratory quotient and fat oxidation in severe obesity and type 2 diabetes. J Clin Invest. 1998 102(7):1345-51.

Argyropoulos G, Harper ME. Uncoupling proteins and thermoregulation. J Appl Physiol. 2002 92(5):2187-98.

Arsenijevic D, Onuma H, Pecqueur C, Raimbault S, Manning BS, Miroux B, Couplan E, Alves-Guerra MC, Goubern M, Surwit R, Bouillaud F, Richard D, Collins S, Ricquier D. Disruption of the uncoupling protein-2 gene in mice reveals a role in immunity and reactive oxygen species production. Nat Genet. 2000 26(4):435-9.

Baffy G. Uncoupling protein-2 and non-alcoholic fatty liver disease. Front Biosci. 2005 10:2082-96.

Batterham RL, Cowley MA, Small CJ, Herzog H, Cohen MA, Dakin CL, Wren AM, Brynes AE, Low MJ, Ghatei MA, Cone RD, Bloom SR. Gut hormone PYY(3-36) physiologically inhibits food intake. Nature. 2002 418(6898):650-4.

Bier DM, Leake RD, Haymond MW, Arnold KJ, Gruenke LD, Sperling MA, Kipnis DM. Measurement of "true" glucose production rates in infancy and childhood with 6,6-dideuteroglucose. Diabetes. 1977 26(11):1016-23.

Bontemps F, Hue L, Hers HG. Phosphorylation of glucose in isolated rat hepatocytes. Sigmoidal kinetics explained by the activity of glucokinase alone. Biochem J. 1978 174(2):603-11.

Boss O, Samec S, Paoloni-Giacobino A, Rossier C, Dulloo A, Seydoux J, Muzzin P, Giacobino JP. Uncoupling protein-3: a new member of the mitochondrial carrier family with tissue-specific expression. FEBS Lett. 1997 408(1):39-42.

Bouchard C, Tremblay A, Després JP, Nadeau A, Lupien PJ, Thériault G, Dussault J, Moorjani S, Pinault S, Fournier G. The response to long-term overfeeding in identical twins. N Engl J Med. 1990 24;322(21):1477-82.

Bouchard C, Tremblay A, Després JP, Thériault G, Nadeau A, Lupien PJ, Moorjani S, Prudhomme D, Fournier G. The response to exercise with constant energy intake in identical twins. Obes Res. 1994 2(5):400-10.

Bouchard C. Defining the genetic architecture of the predisposition to obesity: a challenging but not insurmountable task. Am J Clin Nutr. 2010 91(1):5-6.

Bouillaud F, Ricquier D, Thibault J, Weissenbach J. Molecular approach to thermogenesis in brown adipose tissue: cDNA cloning of the mitochondrial uncoupling protein. Proc Natl Acad Sci U S A. 1985 82(2):445-8.

Brand MD, Esteves TC. Physiological functions of the mitochondrial uncoupling proteins UCP2 and UCP3. Cell Metab. 2005 2(2):85-93.

Briggs DI, Andrews ZB. A recent update on the role of ghrelin in glucose homeostasis. Curr Diabetes Rev. 2011 7(3):201-7.

Brooke MH, Kaiser KK. Muscle fiber types: how many and what kind? Arch Neurol. 1970 23(4):369-79.

Cadenas S, Buckingham JA, Samec S, Seydoux J, Din N, Dulloo AG, Brand MD. UCP2 and UCP3 rise in starved rat skeletal muscle but mitochondrial proton conductance is unchanged. FEBS Lett. 1999 462(3):257-60.

Cadenas S, Buckingham JA, St-Pierre J, Dickinson K, Jones RB, Brand MD. AMP decreases the efficiency of skeletal-muscle mitochondria. Biochem J. 2000 351 Pt 2:307-11.

Cannon B, Houstek J, Nedergaard J. Brown adipose tissue. More than an effector of thermogenesis? Ann N Y Acad Sci. 1998 856:171-87.

Cantó C, Jiang LQ, Deshmukh AS, Mataki C, Coste A, Lagouge M, Zierath JR, Auwerx J. Interdependence of AMPK and SIRT1 for metabolic adaptation to fasting and exercise in skeletal muscle. Cell Metab. 2010 11(3):213-9.

Cassell PG, Saker PJ, Huxtable SJ, Kousta E, Jackson AE, Hattersley AT, Frayling TM, Walker M, Kopelman PG, Ramachandran A, Snehelatha C, Hitman GA, McCarthy MI. Evidence that single nucleotide polymorphism in the uncoupling protein 3 (UCP3) gene influences fat distribution in women of European and Asian origin. Diabetologia. 2000 43(12):1558-64.

Clarke IJ, Henry BA. Targeting energy expenditure in muscle as a means of combating obesity. Clin Exp Pharmacol Physiol. 2010 37(1):121-4.

Costford SR, Crawford SA, Dent R, McPherson R, Harper ME. Increased susceptibility to oxidative damage in post-diabetic human myotubes. Diabetologia. 2009 52(11):2405-15.

Costill DL, Daniels J, Evans W, Fink W, Krahenbuhl G, Saltin B. Skeletal muscle enzymes and fiber composition in male and female track athletes. J Appl Physiol. 1976 40(2):149-54.

Cypess AM, Lehman S, Williams G, Tal I, Rodman D, Goldfine AB, Kuo FC, Palmer EL, Tseng YH, Doria A, Kolodny GM, Kahn CR. Identification and importance of brown adipose tissue in adult humans. N Engl J Med. 2009 360(15):1509-17.

Dalgaard LT, Sørensen TI, Drivsholm T, Borch-Johnsen K, Andersen T, Hansen T, Pedersen O. A prevalent polymorphism in the promoter of the UCP3 gene and its relationship to body mass index and long term body weight change in the Danish population. J Clin Endocrinol Metab. 2001 86(3):1398-402.

DeFronzo RA, Ferrannini E, Sato Y, Felig P, Wahren J. Synergistic interaction between exercise and insulin on peripheral glucose uptake. J Clin Invest. 1981 68(6):1468-74.

Dent RM, Penwarden RM, Harris N, Hotz SB. Development and evaluation of patient-centered software for a weight-management clinic. Obes Res. 2002 10(7):651-6.

Dombrowski GJ Jr, Swiatek KR, Chao KL. Lactate, 3-hydroxybutyrate, and glucose as substrates for the early postnatal rat brain. Neurochem Res. 1989 14(7):667-75.

Echtay KS, Esteves TC, Pakay JL, Jekabsons MB, Lambert AJ, Portero-Otín M, Pamplona R, Vidal-Puig AJ, Wang S, Roebuck SJ, Brand MD. A signalling role for 4-hydroxy-2-nonenal in regulation of mitochondrial uncoupling. EMBO J. 2003 22(16):4103-10.

Echtay KS, Roussel D, St-Pierre J, Jekabsons MB, Cadenas S, Stuart JA, Harper JA, Roebuck SJ, Morrison A, Pickering S, Clapham JC, Brand MD. Superoxide activates mitochondrial uncoupling proteins. Nature. 2002 415(6867):96-9.

Elchuri S, Oberley TD, Qi W, Eisenstein RS, Jackson Roberts L, Van Remmen H, Epstein CJ, Huang TT. CuZnSOD deficiency leads to persistent and widespread oxidative damage and hepatocarcinogenesis later in life. Oncogene. 2005 24(3):367-80.

El-Khoury TG, Bahr GM, Echtay KS. Muramyl-dipeptide-induced mitochondrial proton leak in macrophages is associated with upregulation of uncoupling protein 2 and the production of reactive oxygen and reactive nitrogen species. FEBS J. 2011 278(17):3054-64.

Enerbäck S, Jacobsson A, Simpson EM, Guerra C, Yamashita H, Harper ME, Kozak LP. Mice lacking mitochondrial uncoupling protein are cold-sensitive but not obese. Nature. 1997 387(6628):90-4.

Erecinska M, Cherian S, Silver IA. Energy metabolism in mammalian brain during development. Prog Neurobiol. 2004 73(6):397-445.

Fang H, Chen M, Ding Y, Shang W, Xu J, Zhang X, Zhang W, Li K, Xiao Y, Gao F, Shang S, Li JC, Tian XL, Wang SQ, Zhou J, Weisleder N, Ma J, Ouyang K, Chen J, Wang X, Zheng M, Wang W, Zhang X, Cheng H. Imaging superoxide flash and metabolism-coupled mitochondrial permeability transition in living animals. Cell Res. 2011 21(9):1295-304.

Farooqi IS, O'Rahilly S. Monogenic human obesity syndromes. Recent Prog Horm Res. 2004;59:409-24.

Feero WG, Guttmacher AE, Collins FS. Genomic medicine--an updated primer. N Engl J Med. 2010 27;362(21):2001-11.

Feldmann HM, Golozoubova V, Cannon B, Nedergaard J. UCP1 ablation induces obesity and abolishes diet-induced thermogenesis in mice exempt from thermal stress by living at thermoneutrality. Cell Metab. 2009 9(2):203-9.

Fink WJ, Costill DL, Pollock ML. Submaximal and maximal working capacity of elite distance runners. Part II. Muscle fiber composition and enzyme activities. Ann N Y Acad Sci.1977 301:323-7.

Fleury C, Neverova M, Collins S, Raimbault S, Champigny O, Levi-Meyrueis C, Bouillaud F, Seldin MF, Surwit RS, Ricquier D, Warden CH. Uncoupling protein-2: a novel gene linked to obesity and hyperinsulinemia. Nat Genet. 1997 15(3):269-72.

Frayling TM, Timpson NJ, Weedon MN, Zeggini E, Freathy RM, Lindgren CM, Perry JR, Elliott KS, Lango H, Rayner NW, Shields B, Harries LW, Barrett JC, Ellard S, Groves CJ, Knight B, Patch AM, Ness AR, Ebrahim S, Lawlor DA, Ring SM, Ben-ShlomoY, Jarvelin MR, Sovio U, Bennett AJ, Melzer D, Ferrucci L, Loos RJ, Barroso I,Wareham NJ, Karpe F, Owen KR, Cardon LR, Walker M, Hitman GA, Palmer CN, Doney AS, Morris AD, Smith GD, Hattersley AT, McCarthy MI. A common variant in the FTO gene is associated with body mass index and predisposes to childhood and adult obesity. Science. 2007 11;316(5826):889-94.

Friedman JM. Obesity. Brown fat and yellow mice. Nature. 1993 23-30;366(6457):720-1.

Fulco M, Schiltz RL, Iezzi S, King MT, Zhao P, Kashiwaya Y, Hoffman E, Veech RL, Sartorelli V. Sir2 regulates skeletal muscle differentiation as a potential sensor of the redox state. Mol Cell. 2003 12(1):51-62.

Fumeron F, Durack-Bown I, Betoulle D, Cassard-Doulcier AM, Tuzet S, Bouillaud F, Melchior JC, Ricquier D, Apfelbaum M. Polymorphisms of uncoupling protein (UCP) and beta 3 adrenoreceptor genes in obese people submitted to a low calorie diet. Int J Obes Relat Metab Disord. 1996 20(12):1051-4.

Gardiner JV, Jayasena CN, Bloom SR. Gut hormones: a weight off your mind. J Neuroendocrinol. 2008 20(6):834-41.

Gaster M, Beck-Nielsen H. The reduced insulin-mediated glucose oxidation in skeletal muscle from type 2 diabetic subjects may be of genetic origin--evidence from cultured myotubes. Biochim Biophys Acta. 2004 1690(1):85-91.

Gaster M, Petersen I, Højlund K, Poulsen P, Beck-Nielsen H. The diabetic phenotype is conserved in myotubes established from diabetic subjects: evidence for primary defects in glucose transport and glycogen synthase activity. Diabetes. 2002 51(4):921-7.

Gatlik-Landwojtowicz E, Aänismaa P, Seelig A. The rate of P-glycoprotein activation depends on the metabolic state of the cell. Biochemistry. 2004 43(46):14840-51.

Gautron L, Elmquist JK. Sixteen years and counting: an update on leptin in energy balance. J Clin Invest. 2011 121(6):2087-93.

Gerrits MF, Ghosh S, Kavaslar N, Hill B, Tour A, Seifert EL, Beauchamp B, Gorman S, Stuart J, Dent R, McPherson R, Harper ME. Distinct skeletal muscle fiber characteristics and gene expression in diet-sensitive versus diet-resistant obesity. J Lipid Res. 2010 51(8):2394-404.

Ghosh S, Dent R, Harper ME, Gorman SA, Stuart JS, McPherson R. Gene expression profiling in whole blood identifies distinct biological pathways associated with obesity. BMC Med Genomics. 2010 3:56.

Gill M, France J, Summers M, McBride BW, Milligan LP. Simulation of the energy costs associated with protein turnover and Na+,K+-transport in growing lambs. J Nutr. 1989 119(9):1287-99.

Gong DW, Monemdjou S, Gavrilova O, Leon LR, Marcus-Samuels B, Chou CJ, Everett C, Kozak LP, Li C, Deng C, Harper ME, Reitman ML. Lack of obesity and normal response to fasting and thyroid hormone in mice lacking uncoupling protein-3. J Biol Chem. 2000 275(21):16251-7.

Hainer V, Stunkard A, Kunesová M, Parízková J, Stich V, Allison DB. A twin study of weight loss and metabolic efficiency. Int J Obes Relat Metab Disord. 2001 25(4):533-7.

Hainer V, Stunkard AJ, Kunesová M, Parízková J, Stich V, Allison DB. Intrapair resemblance in very low calorie diet-induced weight loss in female obese identical twins. Int J Obes Relat Metab Disord. 2000 24(8):1051-7.

Halaas JL, Gajiwala KS, Maffei M, Cohen SL, Chait BT, Rabinowitz D, Lallone RL, Burley SK, Friedman JM. Weight-reducing effects of the plasma protein encoded by the obese gene. Science. 1995 269(5223):543-6.

Harper ME, Dent R, Monemdjou S, Bézaire V, Van Wyck L, Wells G, Kavaslar GN, Gauthier A, Tesson F, McPherson R. Decreased mitochondrial proton leak and reduced expression of uncoupling protein 3 in skeletal muscle of obese diet-resistant women. Diabetes. 2002 51(8):2459-66.

Harper ME, Green K, Brand MD. The efficiency of cellular energy transduction and its implications for obesity. Annu Rev Nutr. 2008;28:13-33.

Hebebrand J. Putting the greater dimensions of obesity into perspective. Obes Facts. 2010 3(6):341-2.

Henry RR, Abrams L, Nikoulina S, Ciaraldi TP. Insulin action and glucose metabolism in nondiabetic control and NIDDM subjects. Comparison using human skeletal muscle cell cultures. Diabetes. 1995 44(8):936-46.

Hirasaka K, Lago CU, Kenaston MA, Fathe K, Nowinski SM, Nikawa T, Mills EM. Identification of a Redox-Modulatory Interaction Between Uncoupling Protein 3 and Thioredoxin 2 in the Mitochondrial Intermembrane Space. Antioxid Redox Signal. 2011

Holmes JM, Hilber K, Galler S, Neil DM. Shortening properties of two biochemically defined muscle fibre types of the Norway lobster Nephrops norvegicus L. J Muscle Res Cell Motil. 1999 20(3):265-78.

Houstis N, Rosen ED, Lander ES. Reactive oxygen species have a causal role in multiple forms of insulin resistance. Nature. 2006 440(7086):944-8.

Huxley H, Hanson J. Changes in the cross-striations of muscle during contraction and stretch and their structural interpretation. Nature. 1954 173(4412):973-6.

Huxley AF, Niedergerke R. Structural changes in muscle during contraction; interference microscopy of living muscle fibres. Nature. 1954 173(4412):971-3.

Jia JJ, Tian YB, Cao ZH, Tao LL, Zhang X, Gao SZ, Ge CR, Lin QY, Jois M. The polymorphisms of UCP1 genes associated with fat metabolism, obesity and diabetes. Mol Biol Rep. 2010 37(3):1513-22.

Kahn CB. Myth: insulin sliding scales work. Med Health R I. 2000 83(9):282-3.

Katz J, Wals PA, Rognstad R. Glucose phosphorylation, glucose-6-phosphatase, and recycling in rat hepatocytes. J Biol Chem. 1978 253(13):4530-6.

Klingenberg M. The ADP and ATP transport in mitochondria and its carrier. Biochim Biophys Acta. 2008 1778(10):1978-2021.

Kojima M, Hosoda H, Date Y, Nakazato M, Matsuo H, Kangawa K. Ghrelin is a growth-hormone-releasing acylated peptide from stomach. Nature. 1999 402(6762):656-60.

Kopelman PG. Obesity as a medical problem. Nature. 2000 6;404(6778):635-43.

Kotliar N, Pilch PF. Expression of the glucose transporter isoform GLUT 4 is insufficient to confer insulin-regulatable hexose uptake to cultured muscle cells. Mol Endocrinol. 1992 6(3):337-45.

Kuang S, Chargé SB, Seale P, Huh M, Rudnicki MA. Distinct roles for Pax7 and Pax3 in adult regenerative myogenesis. J Cell Biol. 2006 172(1):103-13.

Larrouy D, Barbe P, Valle C, Déjean S, Pelloux V, Thalamas C, Bastard JP, Le Bouil A, Diquet B, Clément K, Langin D, Viguerie N. Gene expression profiling of human skeletal muscle in response to stabilized weight loss. Am J Clin Nutr. 2008 88(1):125-32.

Le Grand F, Rudnicki MA. Skeletal muscle satellite cells and adult myogenesis. Curr Opin Cell Biol. 2007 19(6):628-33.

Lefort N, Glancy B, Bowen B, Willis WT, Bailowitz Z, De Filippis EA, Brophy C, Meyer C, Højlund K, Yi Z, Mandarino LJ. Increased reactive oxygen species production and lower abundance of complex I subunits and carnitine palmitoyltransferase 1B protein despite normal mitochondrial respiration in insulin-resistant human skeletal muscle. Diabetes. 2010 59(10):2444-52.

Lenz A, Diamond FB Jr. Obesity: the hormonal milieu. Curr Opin Endocrinol Diabetes Obes. 2008 15(1):9-20.

Levine JA, Eberhardt NL, Jensen MD. Role of nonexercise activity thermogenesis in resistance to fat gain in humans. Science. 1999 283(5399):212-4.

Levine JA. Non-exercise activity thermogenesis (NEAT). Best Pract Res Clin Endocrinol Metab. 2002 16(4):679-702.

Levine JA. Nonexercise activity thermogenesis--liberating the life-force. J Intern Med. 2007 262(3):273-87.

Li Y, Huang TT, Carlson EJ, Melov S, Ursell PC, Olson JL, Noble LJ, Yoshimura MP, Berger C, Chan PH, Wallace DC, Epstein CJ. Dilated cardiomyopathy and neonatal lethality in mutant mice lacking manganese superoxide dismutase. Nat Genet. 1995 11(4):376-81.

Lillioja S, Young AA, Culter CL, Ivy JL, Abbott WG, Zawadzki JK, Yki-Järvinen H, Christin L, Secomb TW, Bogardus C. Skeletal muscle capillary density and fiber type are possible determinants of in vivo insulin resistance in man. J Clin Invest. 1987 80(2):415-24.

Lin B, Coughlin S, Pilch PF. Bidirectional regulation of uncoupling protein-3 and GLUT-4 mRNA in skeletal muscle by cold. Am J Physiol. 1998 275(3 Pt1):E386-91.

Liu YJ, Liu PY, Long J, Lu Y, Elze L, Recker RR, Deng HW. Linkage and association analyses of the UCP3 gene with obesity phenotypes in Caucasian families. Physiol Genomics. 2005 22(2):197-203.

Mailloux RJ, Seifert EL, Bouillaud F, Aguer C, Collins S, Harper ME. Glutathionylation acts as a control switch for uncoupling proteins UCP2 and UCP3. J Biol Chem. 2011a 286(24):21865-75.

Mailloux RJ, Adjeitey CN, Xuan JY, Harper ME. Crucial yet divergent roles of mitochondrial redox state in skeletal muscle vs. brown adipose tissue energetics. FASEB J. 2011b

Mailloux RJ, Harper ME. Uncoupling proteins and the control of mitochondrial reactive oxygen species production. Free Radic Biol Med. 2011c 51(6):1106-15.

Mann T, Tomiyama AJ, Westling E, Lew AM, Samuels B, Chatman J. Medicare's search for effective obesity treatments: diets are not the answer. Am Psychol. 2007 62(3):220-33.

Marx J. Cellular warriors at the battle of the bulge. Science. 2003 7;299(5608):846-9.

Mauro A. Satellite cell of skeletal muscle fibers. J Biophys Biochem Cytol. 1961 9:493-5.

Meugnier E, Bossu C, Oliel M, Jeanne S, Michaut A, Sothier M, Brozek J, Rome S, Laville M, Vidal H. Changes in gene expression in skeletal muscle in response to fat overfeeding in lean men. Obesity (Silver Spring). 2007 15(11):2583-94.

Morgello S, Uson RR, Schwartz EJ, Haber RS. The human blood-brain barrier glucose transporter (GLUT1) is a glucose transporter of gray matter astrocytes. Glia. 1995 14(1):43-54.

Mouly V, Edom F, Barbet JP, Butler-Browne GS. Plasticity of human satellite cells. Neuromuscul Disord. 1993 3(5-6):371-7.

Muller FL, Liu Y, Van Remmen H. Complex III releases superoxide to both sides of the inner mitochondrial membrane. J Biol Chem. 2004 279(47):49064-73.

Murphy JE, Porter RK. The control of oxidative phosphorylation in the adrenal gland (Y1) cell line. Adv Exp Med Biol. 2009;645:35-41.

Nadtochiy SM, Tompkins AJ, Brookes PS. Different mechanisms of mitochondrial proton leak in ischaemia/reperfusion injury and preconditioning: implications for pathology and cardioprotection. Biochem J. 2006 395(3):611-8.

Nedachi T, Kadotani A, Ariga M, Katagiri H, Kanzaki M. Ambient glucose levels qualify the potency of insulin myogenic actions by regulating SIRT1 and FoxO3a in C2C12 myocytes. Am J Physiol Endocrinol Metab. 2008 294(4):E668-78.

Neel JV. Diabetes mellitus: a "thrifty" genotype rendered detrimental by "progress"? Am J Hum Genet. 1962 14:353-62.

Nègre-Salvayre A, Hirtz C, Carrera G, Cazenave R, Troly M, Salvayre R, Pénicaud L, Casteilla L. A role for uncoupling protein-2 as a regulator of mitochondrial hydrogen peroxide generation. FASEB J. 1997 11(10):809-15.

Nishikawa T, Edelstein D, Du XL, Yamagishi S, Matsumura T, Kaneda Y, Yorek MA, Beebe D, Oates PJ, Hammes HP, Giardino I, Brownlee M. Normalizing mitochondrial superoxide production blocks three pathways of hyperglycaemic damage. Nature. 2000 404(6779):787-90.

Nobes CD, Brown GC, Olive PN, Brand MD. Non-ohmic proton conductance of the mitochondrial inner membrane in hepatocytes. J Biol Chem. 1990 265(22):12903-9.

Obesity and Overweight Fact sheet N°311 Updated March 2011

http://www.who.int/mediacentre/factsheets/fs311/en/

Pette D, Staron RS. Mammalian skeletal muscle fiber type transitions. Int Rev Cytol. 1997;170:143-223.

Pierre JL, Fontecave M. Iron and activated oxygen species in biology: the basic chemistry. Biometals. 1999 12(3):195-9.

Porter RK, Brand MD. Body mass dependence of H+ leak in mitochondria and its relevance to metabolic rate. Nature. 1993 362(6421):628-30.

Pouvreau S. Superoxide flashes in mouse skeletal muscle are produced by discrete arrays of active mitochondria operating coherently. PLoS One. 20105(9).

Rabkin M, Blum JJ. Quantitative analysis of intermediary metabolism in hepatocytes incubated in the presence and absence of glucagon with a substrate mixture containing glucose, ribose, fructose, alanine and acetate. Biochem J. 1985 225(3):761-86.

Rando TA, Blau HM. Primary mouse myoblast purification, characterization, and transplantation for cell-mediated gene therapy. J Cell Biol. 1994 125(6):1275-87.

Rawson ES, Nolan A, Silver K, Shuldiner AR, Poehlman ET. No effect of the Trp64Arg beta(3)-adrenoceptor gene variant on weight loss, body composition, or energy expenditure in obese, caucasian postmenopausal women. Metabolism. 2002 51(6):801-5.

Reeds PJ, Fuller MF, Cadenhead A, Hay SM. Urea synthesis and leucine turnover in growing pigs: changes during 2 d following the addition of carbohydrate or fat to the diet. Br J Nutr. 1987 58(2):301-11.

Rhee SG, Chang TS, Jeong W, Kang D. Methods for detection and measurement of hydrogen peroxide inside and outside of cells. Mol Cells. 2010 29(6):539-49.

Rial E, Aguirregoitia E, Jiménez-Jiménez J, Ledesma A. Alkylsulfonates activate the uncoupling protein UCP1: implications for the transport mechanism. Biochim Biophys Acta. 2004 1608(2-3):122-30.

Ricquier D, Bouillaud F. The uncoupling protein homologues: UCP1, UCP2, UCP3, StUCP and AtUCP. Biochem J. 2000 345 Pt 2:161-79.

Rolfe DF, Brand MD. Contribution of mitochondrial proton leak to skeletal muscle respiration and to standard metabolic rate. Am J Physiol. 1996 271(4Pt 1):C1380-9.

Rolfe DF, Brown GC. Cellular energy utilization and molecular origin of standard metabolic rate in mammals. Physiol Rev. 1997 77(3):731-58.

Rolfe DF, Hulbert AJ, Brand MD. Characteristics of mitochondrial proton leak and control of oxidative phosphorylation in the major oxygen-consuming tissues of the rat. Biochim Biophys Acta. 1994 1188(3):405-16.

Rolfe DF, Newman JM, Buckingham JA, Clark MG, Brand MD. Contribution of mitochondrial proton leak to respiration rate in working skeletal muscle and liver and to SMR. Am J Physiol. 1999 276(3 Pt 1):C692-9.

Saltin B. The interplay between peripheral and central factors in the adaptive response to exercise and training. Ann N Y Acad Sci. 1977;301:224-31.

Sargeant RJ, Pâquet MR. Effect of insulin on the rates of synthesis and degradation of GLUT1 and GLUT4 glucose transporters in 3T3-L1 adipocytes. Biochem J. 1993 290 (Pt 3):913-9.

Schantz PG, Henriksson J. Enzyme levels of the NADH shuttle systems: measurements in isolated muscle fibres from humans of differing physical activity. Acta Physiol Scand. 1987 129(4):505-15.

Schrauwen P, Xia J, Bogardus C, Pratley RE, Ravussin E. Skeletal muscle uncoupling protein 3 expression is a determinant of energy expenditure in Pima Indians. Diabetes. 1999 48(1):146-9.

Schuler M, Ali F, Chambon C, Duteil D, Bornert JM, Tardivel A, Desvergne B, Wahli W, Chambon P, Metzger D. PGC1alpha expression is controlled in skeletal muscles by PPARbeta, whose ablation results in fiber-type switching, obesity, and type 2 diabetes. Cell Metab. 2006 4(5):407-14.

Schwartz J, Huo JS, Piwien-Pilipuk G. Growth hormone regulated gene expression. Minerva Endocrinol. 2002 27(4):231-41.

Schwarz M, Andrade-Navarro MA, Gross A. Mitochondrial carriers and pores: key regulators of the mitochondrial apoptotic program? Apoptosis. 2007 12(5):869-76.

Seifert EL, Fiehn O, Bezaire V, Bickel DR, Wohlgemuth G, Adams SH, Harper ME. Long-chain fatty acid combustion rate is associated with unique metabolite profiles in skeletal muscle mitochondria. PLoS One. 2010 5(3):e9834.

Shabalina IG, Hoeks J, Kramarova TV, Schrauwen P, Cannon B, Nedergaard J. Cold tolerance of UCP1-ablated mice: a skeletal muscle mitochondria switch toward lipid oxidation with marked UCP3 up-regulation not associated with increased basal, fatty acid- or ROS-induced uncoupling or enhanced GDP effects. Biochim Biophys Acta. 2010 1797(6-7):968-80.

Shefer G, Wleklinski-Lee M, Yablonka-Reuveni Z. Skeletal muscle satellite cells can spontaneously enter an alternative mesenchymal pathway. J Cell Sci. 2004 117(Pt 22):5393-404.

Shiwaku K, Nogi A, Anuurad E, Kitajima K, Enkhmaa B, Shimono K, Yamane Y. Difficulty in losing weight by behavioral intervention for women with Trp64Arg polymorphism of the beta3-adrenergic receptor gene. Int J Obes Relat Metab Disord. 2003 27(9):1028-36.

Simoneau JA, Bouchard C. Genetic determinism of fiber type proportion in human skeletal muscle. FASEB J. 1995 9(11):1091-5.

Simoneau JA, Kelley DE. Altered glycolytic and oxidative capacities of skeletal muscle contribute to insulin resistance in NIDDM. J Appl Physiol. 1997 83(1):166-71.

Smerdu V, Soukup T. Demonstration of myosin heavy chain isoforms in rat and humans: the specificity of seven available monoclonal antibodies used in immunohistochemical and immunoblotting methods. Eur J Histochem. 2008 52(3):179-90.

Sparks LM, Xie H, Koza RA, Mynatt R, Hulver MW, Bray GA, Smith SR. A high-fat diet coordinately downregulates genes required for mitochondrial oxidative phosphorylation in skeletal muscle. Diabetes. 2005 54(7):1926-33.

Spiegelman BM. PPAR-gamma: adipogenic regulator and thiazolidinedione receptor. Diabetes. 1998 47(4):507-14.

Stock MJ. Gluttony and thermogenesis revisited. Int J Obes Relat Metab Disord. 1999 23(11):1105-17.

Sugioka K, Nakano M, Naito I, Tero-Kubota S, Ikegami Y. Properties of a coenzyme, pyrroloquinoline quinone: generation of an active oxygen species during a reduction-oxidation cycle in the presence of NAD(P)H and O2. Biochim Biophys Acta. 1988 964(2):175-82.

Summers, M., B. W. McBride and L. P. Milligan. 1988. Components of basal energy expenditure. In: A. Dobson and M. J. Dobson (Ed.) Aspects of Digestive Physiology in Ruminants. pp 257-286. Cornell University Press, Ithaca, NY.

Szent-Györgyi AG. The early history of the biochemistry of muscle contraction. J Gen Physiol. 2004 123(6):631-41.

Talbot DA, Lambert AJ, Brand MD. Production of endogenous matrix superoxide from mitochondrial complex I leads to activation of uncoupling protein 3. FEBS Lett. 2004 556(1-3):111-5.

Tanner CJ, Barakat HA, Dohm GL, Pories WJ, MacDonald KG, Cunningham PR, Swanson MS, Houmard JA. Muscle fiber type is associated with obesity and weight loss. Am J Physiol Endocrinol Metab. 2002 282(6):E1191-6.

The International Obesity Task Force (IASO/IOTF) analysis in 2010

http://www.iaso.org/iotf/

Thorleifsson G, Walters GB, Gudbjartsson DF, Steinthorsdottir V, Sulem P, Helgadottir A, Styrkarsdottir U, Gretarsdottir S, Thorlacius S, Jonsdottir I, Jonsdottir T, Olafsdottir EJ, Olafsdottir GH, Jonsson T, Jonsson F, Borch-Johnsen K, Hansen T, Andersen G, Jorgensen T, Lauritzen T, Aben KK, Verbeek AL, Roeleveld N, Kampman E, Yanek LR, Becker LC, Tryggvadottir L, Rafnar T, Becker DM, Gulcher J, Kiemeney LA, Pedersen O, Kong A, Thorsteinsdottir U, Stefansson K. Genome-wide association yields new sequence variants at seven loci that associate with measures of obesity. Nat Genet. 2009 41(1):18-24.

Toime LJ, Brand MD. Uncoupling protein-3 lowers reactive oxygen species production in isolated mitochondria. Free Radic Biol Med. 2010 Aug 49(4):606-11.

Tschöp M, Smiley DL, Heiman ML. Ghrelin induces adiposity in rodents. Nature. 2000 407(6806):908-13.

Turrens JF, Boveris A. Generation of superoxide anion by the NADH dehydrogenase of bovine heart mitochondria. Biochem J. 191(2):421-7.

Ukropcova B, McNeil M, Sereda O, de Jonge L, Xie H, Bray GA, Smith SR. Dynamic changes in fat oxidation in human primary myocytes mirror metabolic characteristics of the donor. J Clin Invest. 2005 115(7):1934-41.

Ukropcova B, Sereda O, de Jonge L, Bogacka I, Nguyen T, Xie H, Bray GA, Smith SR. Family history of diabetes links impaired substrate switching and reduced mitochondrial content in skeletal muscle. Diabetes. 2007 56(3):720-7.

Van Marken Lichtenbelt WD, Vanhommerig JW, Smulders NM, Drossaerts JM, Kemerink GJ, Bouvy ND, Schrauwen P, Teule GJ. Cold-activated brown adipose tissue in healthy men. N Engl J Med. 2009 360(15):1500-8.

Vidal-Puig AJ, Grujic D, Zhang CY, Hagen T, Boss O, Ido Y, Szczepanik A, Wade J, Mootha V, Cortright R, Muoio DM, Lowell BB. Energy metabolism in uncoupling protein 3 gene knockout mice. J Biol Chem. 2000 275(21):16258-66.

Virtanen KA, Lidell ME, Orava J, Heglind M, Westergren R, Niemi T, Taittonen M, Laine J, Savisto NJ, Enerbäck S, Nuutila P. Functional brown adipose tissue in healthy adults. N Engl J Med. 2009 360(15):1518-25.

Vishwasrao HD, Heikal AA, Kasischke KA, Webb WW. Conformational dependence of intracellular NADH on metabolic state revealed by associated fluorescence anisotropy. J Biol Chem. 2005 280(26):25119-26.

Walder K, Norman RA, Hanson RL, Schrauwen P, Neverova M, Jenkinson CP, Easlick J, Warden CH, Pecqueur C, Raimbault S, Ricquier D, Silver MH, Shuldiner AR, Solanes G, Lowell BB, Chung WK, Leibel RL, Pratley R, Ravussin E. Association between uncoupling protein polymorphisms (UCP2-UCP3) and energy metabolism/obesity in Pima indians. Hum Mol Genet. 1998 7(9):1431-5.

Wang W, Fang H, Groom L, Cheng A, Zhang W, Liu J, Wang X, Li K, Han P, Zheng M, Yin J, Wang W, Mattson MP, Kao JP, Lakatta EG, Sheu SS, Ouyang K, Chen J, Dirksen RT, Cheng H. Superoxide flashes in single mitochondria. Cell. 2008 134(2):279-90.

Willer CJ, Speliotes EK, Loos RJ, Li S, Lindgren CM, Heid IM, Berndt SI, Elliott AL, Jackson AU, Lamina C, Lettre G, Lim N, Lyon HN, McCarroll SA, Papadakis K, Qi L, Randall JC, Roccasecca RM,

Sanna S, Scheet P, Weedon MN, Wheeler E, Zhao JH, Jacobs LC, Prokopenko I, Soranzo N, Tanaka T, Timpson NJ, Almgren P, Bennett A, Bergman RN, Bingham SA, Bonnycastle LL, Brown M, Burtt NP, Chines P, Coin L, Collins FS, Connell JM, Cooper C, Smith GD, Dennison EM, Deodhar P, Elliott P, Erdos MR, Estrada K, Evans DM, Gianniny L, Gieger C, Gillson CJ, Guiducci C, Hackett R, Hadley D, Hall AS, Havulinna AS, Hebebrand J, Hofman A, Isomaa B, Jacobs KB, Johnson T, Jousilahti P, Jovanovic Z, Khaw KT, Kraft P, Kuokkanen M, Kuusisto J, Laitinen J, Lakatta EG, Luan J, Luben RN, Mangino M, McArdle WL, Meitinger T, Mulas A, Munroe PB, Narisu N, Ness AR, Northstone K, O'Rahilly S, Purmann C, Rees MG, Ridderstråle M, Ring SM, Rivadeneira F, Ruokonen A, Sandhu MS, Saramies J, Scott LJ, Scuteri A, Silander K, Sims MA, Song K, Stephens J, Stevens S, Stringham HM, Tung YC, Valle TT, Van Duijn CM, Vimaleswaran KS, Vollenweider P, Waeber G, Wallace C, Watanabe RM, Waterworth DM, Watkins N; Wellcome Trust Case Control Consortium, Witteman JC, Zeggini E, Zhai G, Zillikens MC, Altshuler D, Caulfield MJ, Chanock SJ, Farooqi IS, Ferrucci L, Guralnik JM, Hattersley AT, Hu FB, Jarvelin MR, Laakso M, Mooser V, Ong KK, Ouwehand WH, Salomaa V, Samani NJ, Spector TD, Tuomi T, Tuomilehto J, Uda M, Uitterlinden AG, Wareham NJ, Deloukas P, Frayling TM, Groop LC, Hayes RB, Hunter DJ, Mohlke KL, Peltonen L, Schlessinger D, Strachan DP, Wichmann HE, McCarthy MI, Boehnke M, Barroso I, Abecasis GR, Hirschhorn JN; Genetic Investigation of ANthropometric Traits Consortium. Six new loci associated with body mass index highlight a neuronal influence on body weight regulation. Nat Genet. 2009 41(1):25-34.

Woods SC, Lotter EC, McKay LD, Porte D Jr. Chronic intracerebroventricular infusion of insulin reduces food intake and body weight of baboons. Nature. 1979 282(5738):503-5.

Xinli W, Xiaomei T, Meihua P, Song L. Association of a mutation in the beta3-adrenergic receptor gene with obesity and response to dietary intervention in Chinese children. Acta Paediatr. 2001 90(11):1233-7.

Yoshida T, Sakane N, Umekawa T, Sakai M, Takahashi T, Kondo M. Mutation of beta 3-adrenergic-receptor gene and response to treatment of obesity. Lancet. 1995 346(8987):1433-4.

Zurlo F, Larson K, Bogardus C, Ravussin E. Skeletal muscle metabolism is a major determinant of resting energy expenditure. J Clin Invest. 1990 86(5):1423-7.